Framework for Correlating the Effect of Temperature on Nonelectrolyte and Ionic Liquid Activity Coefficients

Timothy C. Frank, Steven G. Arturo, and Bruce S. Holden
Engineering and Process Science, Core R&D, The Dow Chemical Company, Midland, MI 48667 and Collegeville, PA 19426

DOI 10.1002/aic.14557
Published online July 24, 2014 in Wiley Online Library (wileyonlinelibrary.com)

A power-law expression is proposed for correlating the temperature dependence of infinite-dilution activity coefficients (γ_{ij}^{∞}) for nonelectrolyte solute–solvent binary pairs and for pairs including an ionic liquid: $\ln\gamma_{ij}^{\infty}(at\ T)/\ln\gamma_{ij}^{\infty}(at\ T_{ref})=\left(T_{ref}/T\right)^{\theta_{ij}}$, where $\theta_{ij}=0$ for Lewis–Randall ideal solutions, $\theta_{ij}=1$ for classic enthalpy-based Scatchard–Hildebrand regular solution and van Laar models, and $-5<\theta_{ij}<5$ for most real binaries. The exponent θ_{ij} is a function of partial molar excess enthalpy ($\overline{h}_{ij}^{E,\infty}$) and entropy ($\overline{s}_{ij}^{E,\infty}$) such that $\theta_{ij}=1/[1-(T\overline{s}_{ij}^{E,\infty}/\overline{h}_{ij}^{E,\infty})]$. Real binaries are classified into seven types corresponding to distinct domains of γ_{ij}^{∞} and θ_{ij}. The new method provides a framework for correlating phase-equilibrium driven temperature effects for a wide variety of chemical and environmental applications. © 2014 American Institute of Chemical Engineers *AIChE J*, 60: 3675–3690, 2014
Keywords: thermodynamics/classical, liquids, nonelectrolyte, phase equilibrium, ionic liquids

Introduction

Activity coefficients have long been used by chemical engineers and scientists to understand and model liquid solution behavior.[1–8] They are used in modeling phase equilibria for the final design of distillation, extraction, and crystallization processes.[9] They also are applied in early-stage process and product development work to guide the screening of process options and candidate solvents[10–12] and to optimize product formulations including pharmaceuticals,[13] paints,[14] and cleaners.[15] Activity coefficients also find application in emulsion polymerization,[16] liquid-phase reaction,[17] chromatography,[18] and other areas of study where liquid composition is important.[14,19,20] In many cases, the effect of temperature is a key consideration.

In this article, we focus on the infinite-dilution (or limiting) activity coefficient of a nonionic solute i dissolved in solvent j (γ_{ij}^{∞}). Knowledge of γ_{ij}^{∞} and γ_{ji}^{∞} for all binary pairs in a multicomponent mixture allows extrapolation to higher concentrations in mixed solution using well-known excess Gibbs energy expressions such as the Wilson, NRTL, or UNIQUAC equations,[3–8] often with results suitable for initial design studies.[5,21] However, it has long been recognized that extrapolation as a function of temperature using these equations generally is not reliable.[3–5,22–24] In light of this situation, we propose an empirical power-law expression for quantifying the temperature dependence of γ_{ij}^{∞}

$$\ln\gamma_{ij}^{\infty}(\text{at }T)=a_{ij}(T_{\text{ref}}/T)^{\theta_{ij}} \tag{1}$$

where T is temperature in Kelvin and a_{ij} is a constant given by a known reference point, $a_{ij}=\ln\gamma_{ij}^{\infty}$ at $T=T_{\text{ref}}$. The exponent θ_{ij} varies markedly with solute–solvent composition, but for many binaries it is insensitive to change in temperature. Although empirical in nature, we show that θ_{ij} can be related to basic thermodynamic properties of the mixture.

Because of limited temperature-dependent data, in this article we mainly consider temperatures in the range of 0–100°C. This is a common temperature range associated with many chemical process operations, formulated liquid product applications, and environmental phenomena, and it includes standard temperatures used for physical property measurements, so here we refer to it as the normal temperature range. We also largely consider noncolloidal, nonelectrolyte mixtures of low molecular weight, single functional group compounds, although we include a number of glycol ethers, nonionic surfactants, and ionic liquids.

The proposed method is intended as a framework for correlating $\gamma_{ij}^{\infty}=f(T)$ for application-directed screening and modeling purposes. It is modeled in spirit after other data-based classification methods that have proven to be valuable guides. These include Robbins' chart of solute–solvent interactions,[10,25] Godfrey's miscibility numbers used to assess liquid-liquid miscibility for organic binary mixtures,[10,26] and Padovani and Suleiman's method for estimating γ_{ij}^{∞} for organic + water mixtures.[27]

Background

We are concerned with the Lewis–Randall standard-state activity coefficient of nonionic solutes in liquid solution.[4,7,8] Well-known activity coefficient models include UNIFAC and other group contribution models,[3–7] but these generally

Correspondence concerning this article should be addressed to T. C. Frank at tcfrank@dow.com.

do not provide a detailed accounting of temperature dependence. Modified UNIFAC[28–30] and the MOSCED modified regular solution model[31,32] address this situation by including specific temperature-dependent model parameters, but the required databases are not yet fully developed. Other models having some degree of built-in temperature dependence or the option of determining temperature-dependent parameter values include COSMO-RS,[33,34] COSMO-SAC,[34,35] NRTL-SAC,[36] F-SAC,[37] linear solvation energy relationship (LSER) models such as the SPACE model,[5,38] and models based on Hansen solubility parameters.[14,39] Methods used to quantify temperature dependence include those involving correlation of partial molar excess enthalpy (for example, using a LSER expression and Kamlet–Taft molecular descriptors[40]), methods involving combination of an excess Gibbs energy expression with an equation of state,[41,42] and a method involving incorporation of a temperature-dependence parameter related to relative excess enthalpy and entropy directly into the excess Gibbs energy expression.[43,44] Modeling of activity coefficients, excess enthalpy and entropy, and phase equilibrium properties in general are active research areas with a variety of approaches including quantum mechanical charge density calculations,[45,46] molecular modeling and molecular dynamics simulations,[47–53] and phase stability analysis.[53,54] Discussions of the state of the science are given elsewhere.[23,24,42,47]

The limiting activity coefficient γ_{ij}^{∞} characterizes intermolecular interactions of solute i completely surrounded by solvent j and is related to the partial molar excess Gibbs energy of mixing[3–8]

$$RT\ln\gamma_{ij}^{\infty}=\overline{g}_{ij}^{E,\infty}=\overline{h}_{ij}^{E,\infty}-T\overline{s}_{ij}^{E,\infty} \tag{2}$$

where $\overline{g}_{ij}^{E,\infty}=$ partial molar excess Gibbs energy for component i at infinite dilution in solvent j (J/mol), $\overline{h}_{ij}^{E,\infty}=$ partial molar excess enthalpy of mixing for component i at infinite dilution in j (J/mol), $\overline{s}_{ij}^{E,\infty}=$ partial molar excess entropy of mixing for component i at infinite dilution in j (J/mol·K), and $R=$ universal gas constant (8.314 J/mol·K).

A version of the Gibbs–Helmholtz equation may be used to determine the temperature dependence of γ_{ij}^{∞} from knowledge of $\overline{h}_{ij}^{E,\infty}$ [3–8,40,55,56]

$$\left[\frac{\partial\ln\gamma_{ij}^{\infty}}{\partial(1/T)}\right]_{P,x}=\frac{\overline{h}_{ij}^{E,\infty}}{R} \tag{3}$$

In some cases, the value of $\overline{h}_{ij}^{E,\infty}$ is fairly constant over a moderate temperature span and Eq. 3 may be rewritten as

$$\gamma_{ij}^{\infty}\big|_{\text{ at }T_2}\approx\gamma_{ij}^{\infty}\big|_{\text{ at }T_1}\exp\left[\frac{\overline{h}_{ij}^{E,\infty}}{R}\left(\frac{1}{T_2}-\frac{1}{T_1}\right)\right] \tag{4}$$

Compilations of enthalpy of mixing data are available elsewhere.[57–59] In many cases, however, $\overline{h}_{ij}^{E,\infty}$ data are not available, and predicting $\overline{h}_{ij}^{E,\infty}$ with sufficient accuracy presents a difficult challenge. Our new method is proposed as a complementary alternative.

Development

Enthalpic and entropic contributions

Many different types of mixture behavior and temperature dependence are possible depending on the signs and relative magnitudes of $\overline{h}_{ij}^{E,\infty}$ and $\overline{s}_{ij}^{E,\infty}$. For example, with many mixtures of nonpolar or moderately polar small molecules, $\overline{h}_{ij}^{E,\infty}$ is positive (endothermic), $\overline{s}_{ij}^{E,\infty}$ is positive, and the enthalpic term dominates. Systems of this type exhibit activity coefficients greater than unity that decrease with increasing temperature. They approach the behavior of the classic Scatchard–Hildebrand regular solution[3–7] for which $\overline{h}_{ij}^{E,\infty}>0$ and $\overline{s}_{ij}^{E,\infty}=0$. An example is benzene + n-heptane.[4] Conversely, when interactions between dissimilar components result in the formation of attractive intermolecular complexes in solution, and entropic effects are relatively small, the enthalpic term is exothermic ($\overline{h}_{ij}^{E,\infty}<0$) and γ_{ij}^{∞} values will be less than unity and increase with increasing temperature. The binary 2-propanone + trichloromethane is a well-known example.[4,55,60] In other cases involving attractive interactions, significant apparent repulsive interactions also are present such as those due to hydrophobic properties of organic components in water (the tendency for hydrophobic groups to come together to minimize contact with water). For these systems, the entropic effect can dominate; values of γ_{ij}^{∞} are greater than unity even though the value of $\overline{h}_{ij}^{E,\infty}$ is negative due to net exothermic behavior—because excess entropy is significant and negative. Many of these systems exhibit segregation and partial miscibility. Examples include various oxygenated organics dissolved in water.[61–63] For these and other organic + water mixtures, enthalpic and entropic effects can change markedly such that the temperature dependence of γ_{ij}^{∞} switches at some key temperature from increasing in magnitude to decreasing in magnitude with increasing temperature. We will discuss this phenomenon later for C_4–C_7 alcohols dissolved in water, mixtures that undergo a change of this kind at about 50°C.[61]

The properties $\overline{h}_{ij}^{E,\infty}$ and $\overline{s}_{ij}^{E,\infty}$ may be evaluated in terms of the temperature dependence parameter θ_{ij} by applying the derivative in Eq. 3 to Eq. 1. Assuming θ_{ij} is constant over the temperature range of interest, the derivation given in the Appendix yields

$$\overline{h}_{ij}^{E,\infty}=\theta_{ij}RT\ln\gamma_{ij}^{\infty} \tag{5}$$

Partial molar excess entropy at infinite dilution is then obtained from Eq. 2

$$\overline{s}_{ij}^{E,\infty}=(\theta_{ij}-1)R\ln\gamma_{ij}^{\infty} \tag{6}$$

Specific values of $\overline{h}_{ij}^{E,\infty}$ and $\overline{s}_{ij}^{E,\infty}$ can be determined at specific temperatures within the temperature range characterized by θ_{ij}, first by calculating $\ln\gamma_{ij}^{\infty}$ at any temperature T via interpolation or extrapolation of the available data using Eq. 1 and θ_{ij}, and then by inserting $\ln\gamma_{ij}^{\infty}$ at T into Eqs. 5 and 6 to obtain $\overline{h}_{ij}^{E,\infty}$ and $\overline{s}_{ij}^{E,\infty}$ at that temperature. This gives

$$\overline{h}_{ij}^{E,\infty}=\theta_{ij}RT\ln\gamma_{\text{ref}}^{\infty}(T_{\text{ref}}/T)^{\theta_{ij}} \tag{7}$$

and

$$\overline{s}_{ij}^{E,\infty}=(\theta_{ij}-1)R\ln\gamma_{\text{ref}}^{\infty}(T_{\text{ref}}/T)^{\theta_{ij}} \tag{8}$$

The temperature dependence parameter θ_{ij} can be expressed in terms of $\overline{h}_{ij}^{E,\infty}$ and $\overline{s}_{ij}^{E,\infty}$, as well. Substituting Eq. 2 into Eq. 5 and solving for θ_{ij} yields

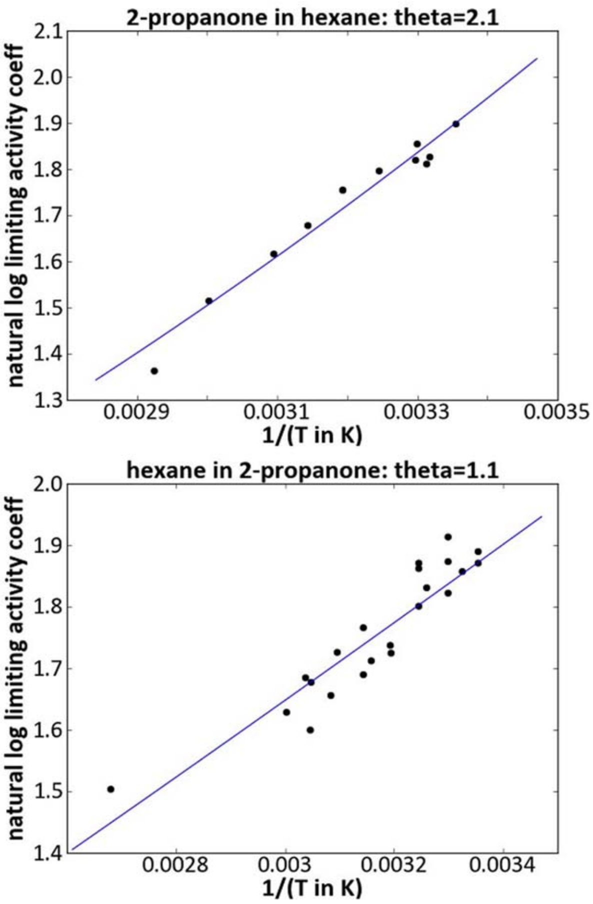

Figure 1. Temperature dependence of γ_{ij}^{∞} data for 2-propanone + hexane (Type II).

The line through the data is the best-fit regression obtained using Eq. 1. Data were taken from the following references: top,[55,64–66]; bottom,[55,64–69]. [Color figure can be viewed in the online issue, which is available at wileyonlinelibrary.com.]

$$\theta_{ij}=\frac{1}{1-(T\overline{s}_{ij}^{E,\infty}/\overline{h}_{ij}^{E,\infty})} \tag{9}$$

Note that the value of θ_{ij} approaches unity (the regular solution model) as the entropic term goes to zero. Fitting temperature-dependent data using a constant value of θ_{ij} amounts to assuming a constant ratio of entropic to enthalpic effects, as shown by rearranging Eq. 9

$$\frac{T\overline{s}_{ij}^{E,\infty}}{\overline{h}_{ij}^{E,\infty}}=\frac{\theta_{ij}-1}{\theta_{ij}} \tag{10}$$

In a number of cases, a constant value of θ_{ij} is able to correlate $\gamma_{i,j}^{\infty}$ over a reasonably wide temperature span of 50–80 Celsius degrees or more (within the normal temperature range). Examples are shown in Figures 1–3. Exceptions include a number of organic + water binaries such as C_4–C_7 alcohols dissolved in water[61] (as discussed earlier), 2-butanone in water, and acetonitrile in water.[57]

In principle, θ_{ij} may be determined *a priori* using methods aimed at calculating $\overline{h}_{ij}^{E,\infty}$ and $\overline{s}_{ij}^{E,\infty}$ from molecular structure and specific molecular interactions. Various methods for calculating $\overline{h}_{ij}^{E,\infty}$ and $\overline{s}_{ij}^{E,\infty}$ are described elsewhere.[46,51,52] It seems that the use of θ_{ij} to model the temperature dependence of $\gamma_{i,j}^{\infty}$ may have an advantage over the usual application of Eqs. 3 and 4 in that only the ratio $T\overline{s}_{ij}^{E,\infty}/\overline{h}_{ij}^{E,\infty}$ need be determined, not the absolute value of $\overline{h}_{ij}^{E,\infty}$, and the ratio may prove to be less sensitive to temperature. It also may be possible to calculate $T\overline{s}_{ij}^{E,\infty}/\overline{h}_{ij}^{E,\infty}$ and thus θ_{ij} as a function of temperature to extend the applicable temperature range when needed. These are questions for future studies.

Both our method and the method of Kaptay for calculating phase diagrams of metallic systems[43,44] treat excess Gibbs energy by including a temperature-dependence parameter that depends on the ratio of excess enthalpy to entropy. However, the specific parameters differ significantly in form and implementation. Our method deals directly with $\gamma_{i,j}^{\infty}$ and is derived using the Gibbs–Helmholtz equation, among other differences.

Mixture types and trends in $\overline{h}_{ij}^{E,\infty}$ and $\overline{s}_{ij}^{E,\infty}$

Most mixtures deviate positively from ideality such that $\gamma_{i,j}^{\infty}>1$. In this case, Eqs. 5–10 indicate three possible domains:

- For $\theta_{ij}>1$, both $\overline{h}_{ij}^{E,\infty}$ and $\overline{s}_{ij}^{E,\infty}$ must be positive. These mixtures are endothermic with a positive change in entropy on mixing. Positive $\overline{s}_{ij}^{E,\infty}$ indicates spontaneous dispersal or spreading of molecules[82] and Gibbs energy[83,84] within the liquid solution.
- For $0<\theta_{ij}<1$, $\overline{h}_{ij}^{E,\infty}$ is positive but $\overline{s}_{ij}^{E,\infty}$ is negative. These mixtures are endothermic with a negative change in entropy. Negative $\overline{s}_{ij}^{E,\infty}$ indicates some degree of segregation (used here to mean the opposite of spreading) in the distribution of molecules and energy.[82–84] Segregation in this sense does not necessarily indicate the formation of a second liquid phase at higher solute concentrations, although it may.
- For $\theta_{ij}<0$, both $\overline{h}_{ij}^{E,\infty}$ and $\overline{s}_{ij}^{E,\infty}$ must be negative. Mixing is exothermic with some degree of segregation.

Our analysis also indicates that for $\gamma_{ij}^{\infty}>1$, a potential domain for which $\overline{h}_{ij}^{E,\infty}$ is negative and $\overline{s}_{ij}^{E,\infty}$ is positive is not allowed. Negative (exothermic) excess enthalpy must be accompanied by some degree of segregation (negative excess entropy) if γ_{ij}^{∞} is to be greater than unity.

In cases with negative deviations from ideality ($0<\gamma_{ij}^{\infty}<1$), the analysis indicates three additional possibilities:

- For $\theta_{ij}>1$, both $\overline{h}_{ij}^{E,\infty}$ and $\overline{s}_{ij}^{E,\infty}$ must be negative. These mixtures are exothermic with segregation.
- For $0<\theta_{ij}<1$, $\overline{h}_{ij}^{E,\infty}$ is negative and $\overline{s}_{ij}^{E,\infty}$ is positive. Mixing is exothermic with spreading.
- For $\theta_{ij}<0$, both $\overline{h}_{ij}^{E,\infty}$ and $\overline{s}_{ij}^{E,\infty}$ must be positive. Mixing is endothermic with spreading.

In addition, for $0<\gamma_{ij}^{\infty}<1$ a potential domain for which $\overline{h}_{ij}^{E,\infty}$ is positive and $\overline{s}_{ij}^{E,\infty}$ is negative is not allowed. Mixing cannot be endothermic with segregation if γ_{ij}^{∞} is to be less than unity.

These results and our assessments regarding trends in γ_{ij}^{∞}, θ_{ij}, $\overline{h}_{ij}^{E,\infty}$, and $\overline{s}_{ij}^{E,\infty}$ provide the basis for a new classification scheme summarized in Table 1. Seven theoretical types of binary mixtures are defined in terms of distinct domains of γ_{ij}^{∞} and θ_{ij}. Type I represents nearly ideal mixtures. Most of the other types approach ideal behavior as temperature increases. Conversely, in those cases where $\theta_{ij}<0$ is observed (Types IV and VII), the mixture moves away from ideal behavior with increasing temperature.

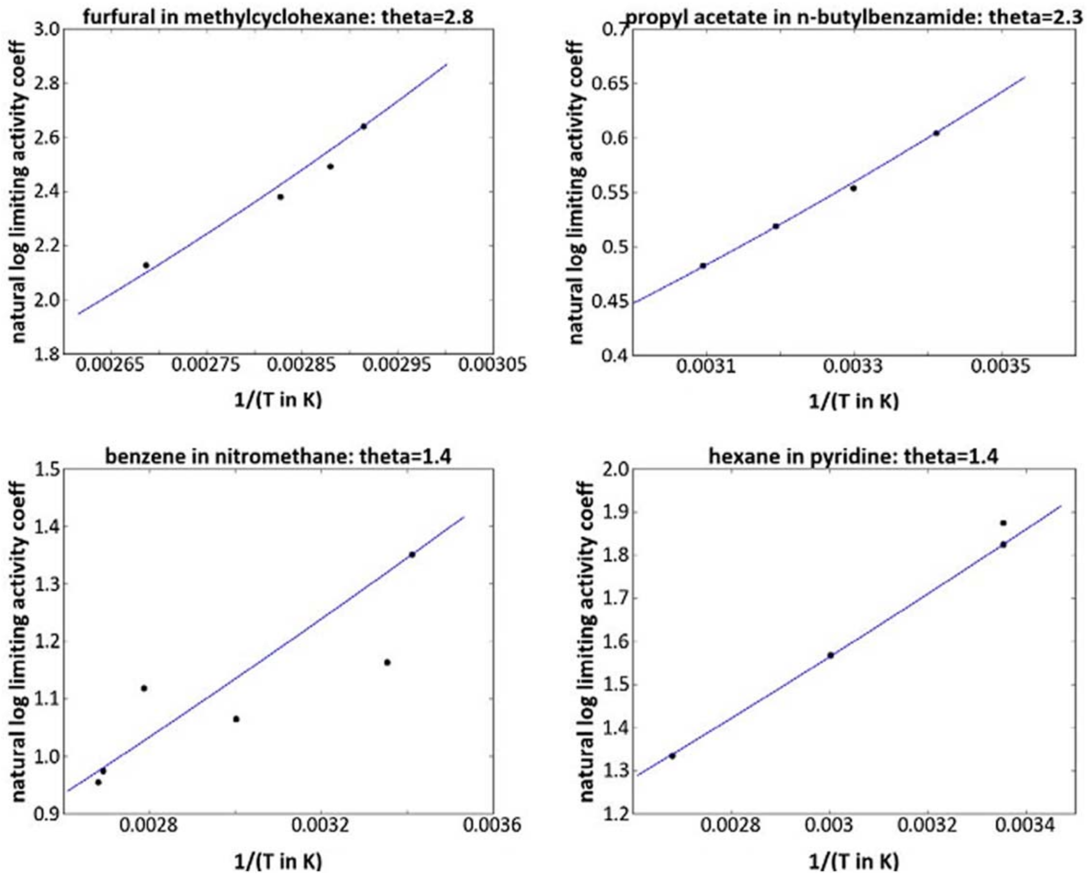

Figure 2. Limiting activity coefficient data vs. temperature for Type II binary pairs.

The line through the data is the best-fit regression obtained using Eq. 1. Data were taken from the following references: top left,[70,71]; top right,[72]; bottom left,[67,70]; bottom right,[67,73]. [Color figure can be viewed in the online issue, which is available at wileyonlinelibrary.com.]

Data Analysis and Initial Correlation

Figure 4 is a plot of $T\bar{s}_{ij}^{E,\infty}$ vs. $\bar{h}_{ij}^{E,\infty}$ obtained by analyzing γ_{ij}^{∞} data available for approximately 500 binary pairs as a function of temperature. The data were obtained from well-known databases[32,57] plus some recent publications (which we cite in subsequent tables and figures). We calculated average values of $\bar{h}_{ij}^{E,\infty}$ using Eq. 4 and then calculated the corresponding value of $\bar{s}_{ij}^{E,\infty}$ from Eq. 2 using the lower temperature for the given dataset. Temperature spans for specific γ_{ij}^{∞} datasets were at least 10 Celsius degrees. Temperatures generally were within the range of 0–100°C, with most of the data between 25°C and 80°C. Datasets were not included if the uncertainty in the γ_{ij}^{∞} measurement was judged to be on the order of the change in γ_{ij}^{∞} with temperature.

In Figure 4, distinct regions and trends are clearly evident, with examples of all the various types listed in Table 1. Figure 4 is an example of the general observation for certain chemical transformations[85] that change in enthalpy and change in entropy are highly correlated. Our classification scheme and the idea that $T\bar{s}_{ij}^{E,\infty}/\bar{h}_{ij}^{E,\infty}$ and θ_{ij} tend to fall within distinct ranges are consistent with these general observations.

Table 2 provides descriptions of typical characteristics for each type and lists typical ranges of γ_{ij}^{∞} and θ_{ij} obtained by analyzing the same database used to generate Figure 4. The results add further definition to the various ranges of θ_{ij} values given in Table 1, although because of limited data, especially for Types IV through VII, the indicated ranges should be considered preliminary.

The θ_{ij} values in Table 2 are the result of specific kinds of solute–solvent interactions affecting $\bar{h}_{ij}^{E,\infty}$ and $\bar{s}_{ij}^{E,\infty}$. Specific interactions that can affect $\bar{h}_{ij}^{E,\infty}$ include static dipole-dipole (polarity effects), induced dipole-dipole, hydrogen bonding (proton donor and proton acceptor interactions), and electron donor/acceptor interactions.[4,86] Factors affecting $\bar{s}_{ij}^{E,\infty}$ include segregation resulting from these interactions, molecular size differences, and the hydrophobic effect[87,88] for organic + water mixtures. Water is included in our classification scheme as a solvent but not as a solute because of the many varied and difficult-to-predict ways water can form hydrogen bonds.

Table 3 lists $\bar{h}_{ij}^{E,\infty}$ and $\bar{s}_{ij}^{E,\infty}$ at standard conditions of 25°C and 60°C for representative binaries. Values were determined by interpolation or extrapolation of the available data using Eqs. 1, 7, and 8. The results reflect the degree of sensitivity to a change in temperature within the normal temperature range. A brief indication of phase equilibrium behavior also is included in Table 3.

To begin probing the relationship between specific interactions and the value of θ_{ij}, we examined the correlation between θ_{ij} and solute–solvent pairings of various classes of organic species (Table 4). We confined our analysis to nonaqueous Type II and III mixtures, as data available for the other types were limited. We considered the following classes of chemical species: (1) active-hydrogen species

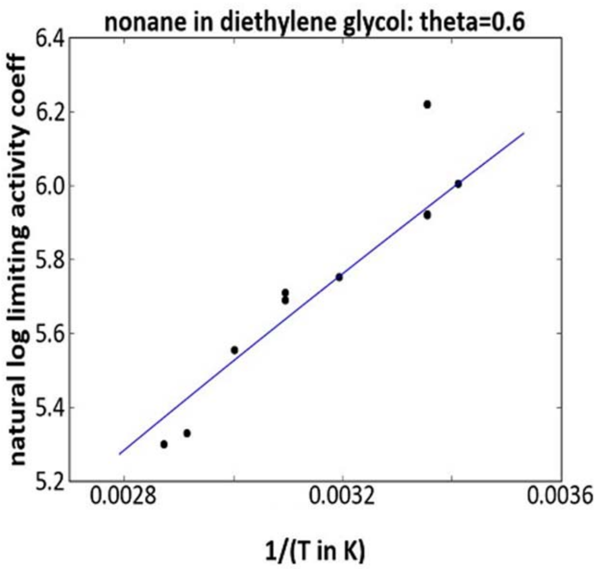

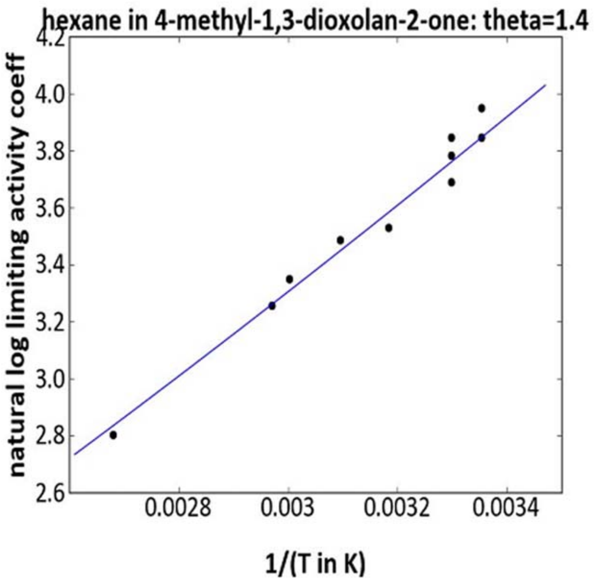

Figure 3. Limiting activity coefficients vs. temperature for nonane in diethylene glycol (Type III) and hexane in 4-methyl-1,3-dioxolan-2-one (Type II).

The line through the data is the best-fit regression obtained using Eq. 1. Data were taken from the following references: top,[74–77]; bottom,[67,78–81]. [Color figure can be viewed in the online issue, which is available at wileyonlinelibrary.com.]

having one or more active hydrogens that may participate in hydrogen bonding, including halogenated organics containing an active hydrogen[4,10,25]; (2) aromatic species involving aromatic rings (with no active hydrogen) with the potential for π-bond interactions; (3) nonpolar species having neither static dipole moment nor aromatic rings; and (4) polar species having a static dipole moment, no aromatic rings, and no active hydrogen. With these assignments, phenol is an active-hydrogen species and benzonitrile is aromatic.

The value of θ reported in Table 4 for a general solute–solvent pairing is the arithmetic mean of all the θ_{ij} values obtained by least squares regression for multiple binaries of the same kind across a wide range of γ_{ij}^{∞} values. We observed that the variability in the resulting set of regressed θ_{ij} values tends to be highest for binaries with relatively low activity coefficient values. Yet, a single average value of θ can be drawn through the data across the entire range of γ_{ij}^{∞} values. This is illustrated in Figure 5, which plots values of θ_{ij} vs. γ_{ij}^{∞} at 20°C for several kinds of solute–solvent pairings.

Figure 6 shows the relationship between experimental γ_{ij}^{∞} values and those calculated using an average θ value for the general solute–solvent pairings listed in Table 4. With this plot, we examine how well the average value of θ represents the temperature dependence of γ_{ij}^{∞} for specific systems. The abscissa is the experimental γ_{ij}^{∞} value corresponding to the highest temperature in the available dataset which ranged from 25 to 180°C. The ordinate is the estimated value of γ_{ij}^{∞} at this highest temperature, calculated via Eq. 1 using the lowest temperature in the dataset and the average θ value for the given mixture class. The interval between the lowest temperature and the highest temperature for a given dataset was 10–155 Celsius degrees. The results show reasonably good representation of γ_{ij}^{∞} as a function of temperature when using the average θ value for a given class, not necessarily the best-fit θ_{ij} value for the specific dataset. The average relative error in γ_{ij}^{∞} was 25.6% or less depending on the solute–solvent class (Table 4). The results of this limited study show the potential for correlating θ_{ij} with molecular structure and specific interactions. This fundamentally involves determining the relationship between molecular interactions and the ratio $T\bar{s}_{ij}^{E,\infty}/\bar{h}_{ij}^{E,\infty}$.

Note that for a given binary $i + j$, the value of θ depends on which component is the solute and which is the solvent; that is, θ_{ij} and θ_{ji} generally are not the same. This depends on which end of the composition range one wishes to consider, in accordance with the well-known fact that a given binary often will exhibit very different values of γ_{ij}^{∞} and γ_{ji}^{∞}.[3–8] For example, consider the temperature dependence of γ^{∞} for the 2-propanone + hexane binary (Figure 1). For 2-propanone dissolved in hexane, a polar solute in a nonpolar solvent, the temperature dependence of $\gamma_{\text{propanone,hexane}}^{\infty}$ is characterized by $\theta_{\text{propanone,hexane}} = 2.1$, close to the average value of 2.3 for this class (Table 4). Conversely, hexane dissolved in 2-propanone is an example of a nonpolar/polar class (average $\theta = 1.4$), and hexane in 2-propanone actually exhibits $\theta_{\text{hexane,propanone}} = 1.1$ (Figure 1). Another example, for the ethanol + 2-propanone binary, is given in Figure 7.

Discussion

Type I. Chemically similar, small molecules

Type I binaries are completely miscible and nearly ideal such that $0.8 < \gamma_{ij}^{\infty} < 1.2$. The effect of γ_{ij}^{∞} on phase equilibrium is small, and the value of θ_{ij} obtained by analyzing available data is uncertain due to significant data scatter. For Type I mixtures, we have assigned θ_{ij} a value of zero because we expect these nearly ideal mixtures to approximate ideal behavior.

Type II. Regular-solution-like

Type II binaries do not form significant attractive or hydrophobic interactions on mixing, so $\bar{h}_{ij}^{E,\infty}$ is positive and $\bar{s}_{ij}^{E,\infty}$ is near zero or positive. Most binaries in our database are Type II mixtures. Examples are shown in Figures 1–3. In analyzing the available data, we found that θ_{ij} falls in the

Table 1. Classification of Activity Coefficient Temperature Dependence

		Change in Quantity with Increasing Temperature			Sign and Trend in Absolute Value (Increasing or Decreasing in Magnitude)		
Mixture Type	γ_{ij}^{∞}, θ_{ij} Range	Temp.	γ_{ij}^{∞}	$\lvert\ln \gamma_{ij}^{\infty}\rvert$ absolute value (magnitude)	$\overline{h}_{ij}^{E,\infty}$	$\overline{s}_{ij}^{E,\infty}$	Comments
$\gamma_{ij}^{\infty} \approx 1$ ($\ln \gamma_{ij}^{\infty}$ is near zero)							
I	$\theta_{ij} \approx 0$	↑	No significant change	≈ 0	≈ 0	≈ 0	Nearly ideal
$\gamma_{ij}^{\infty} > 1$ ($\ln \gamma_{ij}^{\infty}$ is positive)							
II	$\theta_{ij} > 1$	↑	↓	↓	Pos., weak function of temperature	Pos.,↓	$RT\ln \gamma_{i,j}^{\infty} \approx$ constant.
III	$0 < \theta_{ij} < 1$	↑	↓	↓	Pos., weak function of temperature	Neg., ↓	$RT\ln \gamma_{i,j}^{\infty} \approx$ constant.
IV	$\theta_{ij} < 0$	↑	↑	↑	Neg.,↑	Neg., ↑	
$0 < \gamma_{ij}^{\infty} < 1$ ($\ln \gamma_{ij}^{\infty}$ is negative)							
V	$\theta_{ij} > 1$	↑	↑	↓ Approaches 0	Neg., weak function of temperature	Neg., ↓	$RT\ln \gamma_{ij}^{\infty} \approx$ constant.
VI	$0 < \theta_{ij} < 1$	↑	↑	↓ Approaches 0	Neg., weak function of temperature	Pos., ↓	$RT\ln \gamma_{ij}^{\infty} \approx$ constant.
VII	$\theta_{ij} < 0$	↑	↓	↑	Pos., ↑	Pos.,↑	–

range of $1 < \theta_{ij} < 5$. This is greater than $\theta_{ij} = 1$ for a true model regular solution of nonpolar compounds because excess entropy for many real endothermic binaries is positive, resulting in a larger value of θ_{ij}.

Type II mixtures can be either completely miscible or partially miscible, normally with upper critical solution temperature (UCST) behavior.[3–7] Values of γ_{ij}^{∞} can be in the range of roughly $1.2 < \gamma_{ij}^{\infty} < 1000$, but more typically are in the range of $2 < \gamma_{ij}^{\infty} < 100$. A well-known guideline[3–7] indicates incipient phase instability at $\ln \gamma_{ij}^{\infty} \approx 2$ to 3 or $\gamma_{ij}^{\infty} \approx 7$ to 20. Better assessments require more detailed knowledge of the excess Gibbs energy relationship or related properties.[3–7,54] Interestingly, whether a Type II mixture is completely miscible seems to make little difference regarding the range of θ_{ij} values (Table 3).

Type III. Endothermic with negative excess entropy

For Type III binaries, $\overline{h}_{ij}^{E,\infty}$ is positive (or near zero) and $\overline{s}_{ij}^{E,\infty}$ is negative. Values of γ_{ij}^{∞} can vary from about 2 up to the tens of thousands or higher. Systems of this type can be completely miscible, partially miscible, or sparingly miscible. Figure 3 and Table 3 show data for representative binaries. Note that the magnitude of $\overline{s}_{ij}^{E,\infty}$ is greatest for sparingly miscible systems due to a strong hydrophobic effect, yet θ_{ij} (and $T\overline{s}_{ij}^{E,\infty}/\overline{h}_{ij}^{E,\infty}$) fall within the same general range because the greater entropic effect is accompanied by a somewhat larger value of $\overline{h}_{ij}^{E,\infty}$. Also, for C_4–C_7 alcohols dissolved in water, enthalpic and entropic effects change markedly at about 50°C.[61] These mixtures are partially miscible Type III mixtures at $T > 50$°C. At $T < 50$°C, they are Type IV mixtures as discussed below. This change is observed to occur as a fairly sharp break with a change in sign. Thus, the alcohol + water binaries may be placed in certain categories or types according to whether temperature is above or below 50°C, and within each of these categories the value of θ_{ij} is reasonably constant.

Type IV. Exothermic with negative excess entropy

Many Type IV binaries exhibit partial miscibility such that mutual solubility decreases with increasing temperature (inverse temperature dependence). In many cases, the mixture exhibits a lower critical solution temperature (LCST)[3–7] due to attractive intermolecular interactions (negative $\overline{h}_{ij}^{E,\infty}$) accompanied by a high degree of segregation (negative $\overline{s}_{ij}^{E,\infty}$), as discussed by van Konynenburg and Scott in their classification of binary phase diagrams.[107,108] This explains

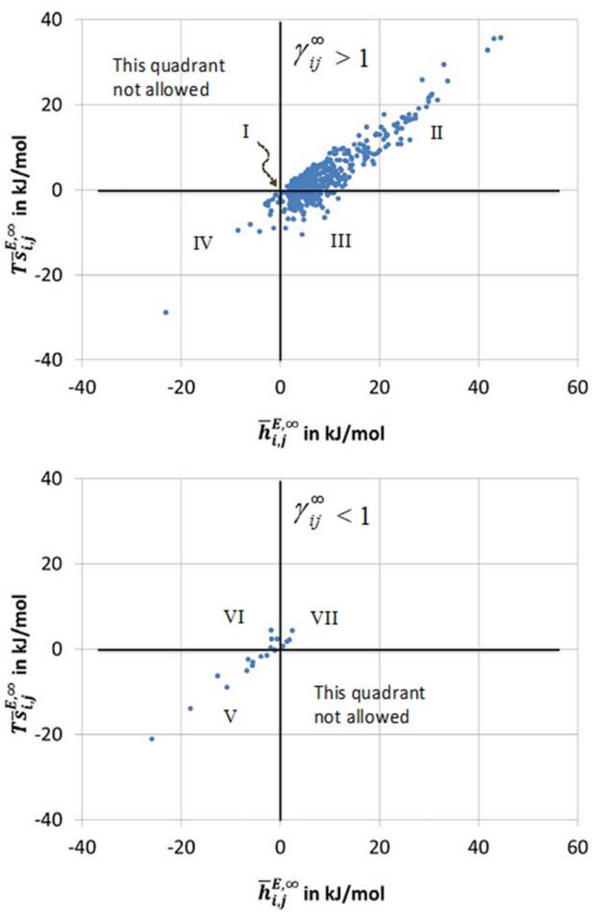

Figure 4. Plots of $\overline{h}_{ij}^{E,\infty}$ and $T\ \overline{s}_{ij}^{E,\infty}$ calculated from $\gamma_{ij}^{\infty} = f(T)$ within the normal temperature range, for $\gamma_{ij}^{\infty} > 1$ (top) and $\gamma_{ij}^{\infty} < 1$ (bottom).

Mixture types (Roman numerals) are defined in Tables 1–3. [Color figure can be viewed in the online issue, which is available at wileyonlinelibrary.com.]

Table 2. Characteristic Behavior from Analysis of Available Data

Mixture Type (from Table 1)	Typical Characteristics	Typical γ_{ij}^{∞} Values[a] and Change with Temperature	Typical θ_{ij} Values[b]
I	Chemically Similar, Small Molecules (Nearly Ideal)	$0.8 < \gamma_{ij}^{\infty} < 1.2$	$\theta_{ij} \approx 0$
II	Regular-Solution-Like	$1.2 < \gamma_{ij}^{\infty} < 1000,\ \frac{\partial \gamma_{ij}^{\infty}}{\partial T} < 0$	$1 < \theta_{ij} < 5$
III	Endothermic with Negative Excess Entropy	$\gamma_{ij}^{\infty} > 2,\ \frac{\partial \gamma_{ij}^{\infty}}{\partial T} < 0$	$0.15 < \theta_{ij} < 1$
IV	Exothermic with Negative Excess Entropy (Inverse Temperature Dependence)	$\gamma_{ij}^{\infty} > 2,\ \frac{\partial \gamma_{ij}^{\infty}}{\partial T} > 0$	$-3 < \theta_{ij} < -0.3$
V	Net Attractive Interactions with Negative Excess Entropy	$0.2 < \gamma_{ij}^{\infty} < 1,\ \frac{\partial \gamma_{ij}^{\infty}}{\partial T} > 0$	$1 < \theta_{ij} < 5$
VI	Net Attractive Interactions with Positive Excess Entropy	$0.2 < \gamma_{ij}^{\infty} < 1,\ \frac{\partial \gamma_{ij}^{\infty}}{\partial T} > 0$	$0.3 < \theta_{ij} < 1$
VII	Chemically Similar, Wide Molecular Size Distribution	$0.6 < \gamma_{ij}^{\infty} < 1,\ \frac{\partial \gamma_{ij}^{\infty}}{\partial T} < 0$	$-5 < \theta_{ij} < -0.5$

[a]As a general rule, phase instability may occur at roughly $\ln \gamma_{ij}^{\infty} \approx 2$ to 3 or $\gamma_{ij}^{\infty} \approx 7$ to 20. See Refs. 3–7 and 54.
[b]Values determined by analysis of data within the normal temperature range of 0–100°C.

why some solutions become cloudy on heating. The temperature at which surfactants exhibit this behavior at a 1 wt % concentration in water is commonly defined as the cloud point. The cloud point temperature normally is higher than the LCST because a 1 wt % concentration is well below the concentration at which the LCST occurs.

Type IV behavior is typical of binaries containing an amphiphilic solute that has both hydrophobic and hydrophilic moieties, often at opposite ends of the molecule, dissolved in water or another hydrogen-bonding polar solvent. LCST behavior may be interpreted as being due to the ability of the hydrophilic end to form hydrogen bonds with the solvent, and this is the dominant effect at temperatures below the LCST, resulting in complete miscibility. As temperature increases, however, the activity coefficient increases in magnitude, and this leads to partial miscibility at some critical temperature.

Many Type IV binaries are mixtures of water with oxygenated organics such as glycol ethers,[98] 2-butanone, and tetrahydrofuran, and nonoxygenates such as triethylamine and nicotine (Table 3). Aqueous mixtures of various nonionic surfactants, polyoxyethylene compounds (polyethers), and polymeric methylcellulose ethers also are well known for exhibiting inverse temperature dependence—in terms of their cloud point behavior. In the case of glycol ethers, the molecule has a hydrophilic hydroxyl end group that can form hydrogen bonds with water and a hydrophobic alkyl ether end group with an entropic repulsion to water. For example, the propylene glycol *n*-butyl ether (PnB) + water binary is characterized by $\gamma_{\mathrm{PnB,water}}^{\infty} = 81$ at 50°C and $\gamma_{\mathrm{PnB,water}}^{\infty} = 130$ at 80°C.[99] Both $\overline{h}_{ij}^{E,\infty}$ and $\overline{s}_{ij}^{E,\infty}$ increase in magnitude with increasing temperature, assuming θ_{ij} is constant (Table 3).

As discussed above, alcohol + water binaries are a special case not easily classified. The C_4–C_7 alcohol + water binaries exhibit Type IV behavior at temperatures below about 50°C (Table 3). This transition may be related to a change in the relative strength of hydrogen bond interactions in alcohol-water complexes.[82,109] Type IV mixtures also include a few nonaqueous small molecule binaries (Table 3), and there are many examples of aqueous and nonaqueous polymer mixtures exhibiting LCST behavior.[110] The fundamentals of LCST behavior are the subject of current research.[53,111,112] Type IV mixtures also can be completely miscible as with C_1–C_3 alcohol + water binaries. Although they differ in terms of phase equilibrium behavior, they exhibit about the same range of θ_{ij} values as the partially miscible binaries (Table 3).

Type V. Net attractive interactions with negative excess entropy

Type V binaries exhibit relatively strong specific intermolecular interactions such that $\gamma_{ij}^{\infty} < 1$, $\overline{h}_{ij}^{E,\infty} < 0$, and $\overline{s}_{ij}^{E,\infty} < 0$. This generally involves formation of new solute–solvent interactions and intermolecular complexes not available to solute in its pure-component state. For example, it is well known that a solute with hydrogen bond-accepting capability but lacking an active hydrogen may form strong attractions with a solvent that possesses an active hydrogen, thereby enabling hydrogen bond donor–acceptor interactions. As discussed earlier, this is the case for 2-propanone (proton acceptor) dissolved in an active-hydrogen compound such as trichloromethane (proton donor and acceptor).[4] The same kind of behavior is observed for trichloromethane dissolved in 2-propanone (Table 3). A similar system is trichloromethane + ethyl acetate (Table 3). Specific attractive interactions of this type also are evident for mixtures of various oxygen or nitrogen-containing organics with the ionic liquid 1-butyl-1-methylpyrrolidinium tricyanomethanide ([BMPYR][TCM])[94] (Table 3). For our purposes, activity coefficients of nonionic solutes dissolved in ionic liquids may be treated the same as nonionic solutes in molecular solvents because the ionic liquid behaves as an ion-pair solvent.[113]

Type VI. Net attractive interactions with positive excess entropy

For Type VI binaries, $\gamma_{ij}^{\infty} < 1$, $\overline{h}_{ij}^{E,\infty} < 0$, and $\overline{s}_{ij}^{E,\infty} > 0$. Both Type V and VI binaries exhibit $\gamma_{ij}^{\infty} < 1$, and γ_{ij}^{∞} increases with increasing temperature. However, characteristic ranges of θ_{ij} values are distinctly different (Tables 1–3). Examples include alcohols dissolved in *N*-methylpyrrolidone polar aprotic solvent and various organics dissolved in trihexyltetradecylphosphonium bis (trifluoromethylsulfonyl) imide ([3C6C14P][BTI]) ionic liquid[101] (Table 3).

Table 3. Properties of Representative Solute–Solvent Binaries

Mixture Type	Binary: Solute	Binary: Solvent	Representative Data: T_{low} (°C)	T_{high} (°C)	γ_{ij}^{∞} at T_{low}	γ_{ij}^{∞} at T_{high}	Calculated Values: θ_{ij} from Eq. 1	$\overline{h}_{ij}^{E,\infty}$ Calculated via Eqs. 1 and 7 kJ/mol at 25°C	$\overline{h}_{ij}^{E,\infty}$ 60°C	$\overline{s}_{ij}^{E,\infty}$ Calculated via Eqs. 1 and 8 J/mol·K at 25°C	$\overline{s}_{ij}^{E,\infty}$ 60°C	$\frac{T\overline{s}_{ij}^{E,\infty}}{\overline{h}_{ij}^{E,\infty}}$ via Eq. 10 Assuming Constant θ_{ij}	Miscibility: Completely Miscible (CM), Upper Critical Solution Temperature (UCST), or Lower Critical Solution Temperature (LCST) Tendency at 0°C to 100°C	γ_{ij}^{∞} Ref.
I	Chemically Similar, Small Molecules													
	Methanol	Diethylene glycol	45	90	0.988	1.02	–	–	–	–	–	–	CM	89
	Ethanol	Methanol	25	64	1.13	1.02	–	–	–	–	–	–	CM	
	Cyclohexane	*n*-heptane	25	70	1.05	1.08	–	–	–	–	–	–	CM	32,57
	Benzene	Toluene	20	40	0.99	0.93	–	–	–	–	–	–	CM	32,57
II	Regular-Solution-Like, Completely Miscible						Pos.	Pos.		Pos.		Pos.		
	Benzene	*n*-heptane	25	100	1.60	1.22	3.8	4.47	3.26	11.1	7.2	0.74	CM	32,57
	Ethanol	2-propanone	25	60	2.45	1.82	3.6	8.07	6.02	19.6	13.1	0.72	CM	Figure 7
	1-chlorobutane	1-tetradecanol	40	75	1.54	1.35	3.4	4.35[a]	3.32	10.3[a]	7.06	0.71	CM	32,57
	n-heptane	Benzene	25	76	2.09	1.59	2.9	5.36	4.33	11.9	8.6	0.66	CM	32,57
	2-propanone	Ethanol	25	80	2.70	1.86	2.8	6.84	5.61	14.7	10.8	0.64	CM	Figure 7
	Ethyl acetate	Hexadecane	20	100	3.1	1.8	2.7	7.27	6.0	15.4	11.4	0.63	CM	32,57
	Benzene	1-methylnaphthalene	20	120	1.31	1.15	2.2	1.45	1.26	2.69	2.10	0.55	CM	32,57
	Propyl acetate	*n*-butylbenzamide	20	50	1.83	1.642	2.3	3.27	2.84[a]	6.14	4.77[a]	0.56	CM	Figure 2
	2-propanone	Hexane	25	60	6.7	4.5	2.1	10.0	8.8	17.6	14.0	0.52	CM	Figure 1
	n-butanol	Diethylene glycol	80	110	2.14	1.90	2.1	5.60[a]	4.96[a]	9.77[a]	7.75[a]	0.52	CM	32,57
	Benzene	Quinoline	20	70	1.67	1.45	2.0	2.51	2.24	4.31	3.43	0.51	CM	32,57
	1,2-dichloroethane	Phenol	50	100	2.44	1.98	1.9	4.76[a]	4.33	7.36[a]	5.99	0.46	CM	32,57
	Ethylbenzene	*N*-methylpyrrolidone	60	90	1.73	1.61	1.6	2.65[a]	2.48	3.44[a]	2.87	0.39	CM	90
	Benzene	Nitromethane	20	100	3.85	2.60	1.4	4.65	4.44	4.67	3.98	0.30	CM	Figure 2
	Hexane	Pyridine	25	100	6.2	3.8	1.4	6.30	6.03	6.95	5.1	0.28	CM	Figure 2
	2-propanone	Methanol	20	70	2.2	1.9	1.3	2.50	2.41	1.96	1.70	0.24	CM	32,57
	Hexane	2-propanone	25	100	6.5	4.3	1.1	5.16	5.09	1.74	1.53	0.10	CM	Figure 1
II	Regular-Solution-Like, Partially-Miscible						Pos.	Pos.		Pos.		Pos.		
	Furfural	Methylcyclohexane	70	100	14	8.2	2.8	26.8[a]	22.0	57.4[a]	42.2	0.64	UCST	Figure 2
	Methanol	*n*-heptane	10	100	150	10	2.8	30.3	24.7	65.5	47.9	0.65	UCST = 57°C	32,57
	Cyclohexane	2-mercaptoethanol	25	60	34.7	16.3	2.2	18.9	16.7	34.1	26.8	0.54	UCST	125
	Cyclohexane	Dimethylsulfoxide	20	70	46	20	1.6	14.4	13.5	17.3	14.6	0.36	UCST	32,57
	Hexane	4-methyl-1,3-dioxolan-2-one	25	100	48	17	1.4	13.4	12.8	12.6	10.8	0.28	UCST	Figure 3
	n-pentane	Triethylene glycol	60	90	33.7	23.2	1.3	13.2[a]	12.7	10.3[a]	8.9	0.24	UCST	89
	n-pentane	Furfural	25	45	20.8	16.8	1.1	8.46	8.34[a]	3.13	2.76[a]	0.11	UCST	92
	n-octane	1,2-ethanediol	25	70	1270	463	1.1	19.2	19.0	5.03	4.46	0.074	UCST	32,57
	Cyclohexane	Ethanol	24	80	11.3	7.6	1.0	6.24	6.21	0.82	0.73	0.038	UCST	93
III	Endothermic with Negative Excess Entropy, Completely Miscible						Pos.	Pos.		Neg.		Neg.		
	Cis−2-pentene	3-methoxypropionitrile	30	70	8.2	6.6	0.88	4.65[a]	4.71	−2.16[a]	−1.66	−0.136	CM[b]	32,57
	Ethylbenzene	*N*-formylmorpholine	60	90	3.46	3.21	0.72	2.41[a]	2.49	−3.1[a]	−2.86	−0.39	CM	90
	Toluene	*n*-butanol	9	100	3.3	2.7	0.66	1.88	1.95	−3.3	−3.0	−0.52	CM[b]	32,57
	Toluene	Methanol	35	69	9.7	8.9	0.37	2.10	2.26	−12.1[a]	−11.6	−1.70	CM[b]	32,57

TABLE 3. *Continued*

Mixture Type	Binary: Solute	Binary: Solvent	Representative Data: T_{low} (°C)	T_{high} (°C)	γ_{ij}^{∞} at T_{low}	γ_{ij}^{∞} at T_{high}	Calculated Values: θ_{ij} from Eq. 1	$\overline{h}_{ij}^{E,\infty}$ Calculated via Eqs. 1 and 7 kJ/mol at 25°C	$\overline{h}_{ij}^{E,\infty}$ 60°C	$\overline{s}_{ij}^{E,\infty}$ Calculated via Eqs. 1 and 8 J/mol·K at 25°C	$\overline{s}_{ij}^{E,\infty}$ 60°C	$\frac{T\overline{s}_{ij}^{E,\infty}}{\overline{h}_{ij}^{E,\infty}}$ via Eq. 10 Assuming Constant θ_{ij}	Miscibility: Completely Miscible (CM), Upper Critical Solution Temperature (UCST), or Lower Critical Solution Temperature (LCST) Tendency at 0°C to 100°C	γ_{ij}^{∞} Ref.
III[e]	Endothermic with Negative Excess Entropy, Partially Miscible						Pos.	Pos.		Neg.		Neg.		
	n-pentane	*N*-formylmorpholine	60	90	19.25	15.3	0.94	7.63[a]	7.68	−1.71[a]	−1.54	−0.064	UCST	90
	Cyclohexane	1,2-ethanediol	20	60	147	90	0.81	9.87	10.1	−7.8	−7.1	−0.23	UCST	32,57
	n-pentane	Diethylene glycol	60	90	70.18	54.19	0.73	8.31[a]	8.57	−10.4[a]	−9.62	−0.37	UCST	89
	n-hexane	Furfural	25	45	25.6	22.2	0.69	5.56	5.76[a]	−8.3	−7.68[a]	−0.45	UCST = 95°C	92
	n-nonane	Diethylene glycol	20	80	405	210	0.62	9.16	9.55	−18.7	−17.4	−0.61	UCST	Figure 3
	n-pentane	[BMPYR][TCM][c]	45	95	16.7	13.4	0.56	4.04[a]	4.24	−10.7[a]	−10.1	−0.79	UCST likely	94
	n-pentane	*N*-methylpyrrolidone	60	90	8.32	7.54	0.55	3.08[a]	3.24	−8.39[a]	−7.89	−0.82	UCST = 52°C	90
	Ethylbenzene	Triethylene glycol	60	90	8.63	7.86	0.51	2.91[a]	3.07	−9.22[a]	−8.71	−0.96	UCST	89
	n-pentanol	Water ($T > 50$°C)	50	100	230	160	0.50	–	7.1	–	−23.2	−1.1	UCST	32,57
	Ethylbenzene	Diethylene glycol	60	90	16.8	15.21	0.42	3.05[a]	3.25	−14.3[a]	−13.7	−1.38	UCST	89
	n-butanol	Water ($T > 50$°C)	50	100	63	50	0.40	–	4.5	–	−20.5	−1.5	UCST = 127°C	32,57
	Isobutanol	Water ($T > 50$°C)	50	98	57	52	0.17	–	1.85	–	−27.9	−4.9	UCST = 133°C	32,57
	2-pentanol	Water ($T > 50$°C)	50	100	129	118	0.13	–	1.7	–	−35.1	−6.7	UCST tendency	32,57
III	Endothermic with Negative Excess Entropy, Sparingly Miscible						Pos.	Pos.		Neg.		Neg.		
	n-heptanol	Water ($T > 50$°C)	50	100	4765	2193	0.67	–	15.4	–	−22.9	−0.5	UCST tendency	32,57
	Anthracene	Water	9	50	5.8E6	1.5E6	0.67	24.9	25.8[a]	−41.2	−38.3[a]	−0.5	UCST tendency	95,96
	Dihydroanthracene	Water	5	40	1.8E6	8.0E5	0.49	16.9	17.9[a]	−59.2	−56.0	−1.0	UCST tendency	95
	m-terphenyl	Water	5	50	1.5E8	4.2E7	0.47	21.3	22.6[a]	−80.1	−76.0[a]	−1.1	UCST tendency	95
	n-octanol	Water	25	100	1.4E4	5900	0.43	10.1	10.7	−45.7	−43.6	−1.3	UCST tendency	32,57
	n-hexanol	Water ($T > 50$°C)	50	70	1193	1000	0.42	–	7.6	–	−35.3	−1.4	UCST tendency	32,57
	Pentane	Water	20	100	1.02E5	3.73E4	0.38	10.7	11.5	−59.2	−56.8	−1.6	UCST tendency	32,57
	Hexane	Water	20	100	3.33E5	1.61E5	0.24	7.7	8.3	−79.6	−77.5	−3.2	UCST tendency	32,57
IV	Exothermic with Negative Excess Entropy, Completely Miscible						Neg.	Neg.		Neg.		Pos.		
	Methanol	Water	25	100	1.67	2.25	−2.0	−2.6	−3.6	−13.0	−16.3	1.5	CM	32,57
	Ethylbenzene	Furfural	25	45	4.52	5.25	−1.5	−5.45	−7.16[a]	−30.82	−30.23[a]	1.7	CM	92
	Ethanol	Water	25	100	3.8	5.6	−1.1	−3.8	−4.8	−23.7	−26.9	1.9	CM	32,57
	Isopropanol	Water	25	100	7.7	13	−1.0	−4.9	−6.0	−33.6	−37.3	2.0	CM	32,57
	Ethylbenzene	[BMPYR][TCM][c]	45	95	2.11	2.29	−0.7	−1.26[a]	−1.52	−10.2[a]	−11.0	2.4	CM	94
	n-propanol	Water	25	100	13.0	17.8	−0.5	−3.3	−3.9	−32.3	−34.2	2.9	CM	32,57
	2-methoxy phenol	1,2,3-trihydroxypropane	Candidate for further study. Temperature range to be determined.											97
IV[f]	Exothermic with Negative Excess Entropy, Partially Miscible						Neg.	Neg.		Neg.		Pos.		
	Tetrahydrofuran	Water	5	55	11	28	−2.0	−13.6	−18.9[a]	−68.5	−85.4[a]	1.5	LCST = 71°C UCST = 138°C	32,57
	2-butanol	Water ($T < 50$°C)	0	50	13.7	35.5	−1.9	−14.1	–	−72.8	–	1.5	LCST = 2°C, UCST = 114°C	32,57
	Propylene glycol *n*-butyl ether	Water	50	80	81	130	−1.2	−11.4[a]	−14.5	−72[a]	−81	1.9	LCST = −10°C	98,99
	n-butanol	Water ($T < 50$°C)	0	50	32.6	63.0	−1.0	−9.7	–	−64.4	–	2.0	LCST = 33°C	32,57

TABLE 3. *Continued*

Mixture Type	Binary: Solute	Binary: Solvent	Representative Data: T_{low} (°C)	T_{high} (°C)	γ_{ij}^{∞} at T_{low}	γ_{ij}^{∞} at T_{high}	Calculated Values: θ_{ij} from Eq. 1	$\overline{h}_{ij}^{E,\infty}$ Calculated via Eqs. 1 and 7 kJ/mol at 25°C	60°C	$\overline{s}_{ij}^{E,\infty}$ Calculated via Eqs. 1 and 8 J/mol·K at 25°C	60°C	$\frac{T\overline{s}_{ij}^{E,\infty}}{\overline{h}_{ij}^{E,\infty}}$ via Eq. 10 Assuming Constant θ_{ij}	Miscibility: Completely Miscible (CM), Upper Critical Solution Temperature (UCST), or Lower Critical Solution Temperature (LCST) Tendency at 0°C to 100°C	γ_{ij}^{∞} Ref.
	2-pentanol	Water ($T < 50$°C)	0	50	59	129	−1.0	−11.6	–	−75.9	–	2.0	slight LCST tendency	32,57
	Dipropylene glycol *n*-butyl ether	Water	50	80	224	360	−0.95	−11.8[a]	−14.6	−81[a]	−90	2.1	LCST ∼ −10°C	98,99
	Isobutanol	Water ($T < 50$°C)	0	50	31.6	57.4	−0.95	−8.8	–	−60.8	–	2.0	LCST tendency	32,57
	Propylene glycol *n*-propyl ether	Water	50	80	46	64	−0.93	−8.2[a]	−10.2	−57[a]	−63	2.1	LCST = 32°C	98,99
	n-pentanol	Water ($T < 50$°C)	0	50	121	230	−0.75	−9.5	–	−74.4	–	2.3	UCST = 188°C	32,57
	n-hexanol	Water ($T < 50$°C)	25	50	885	1193	−0.50	−9.0	–	−86.6	–	3.0	UCST = 225°C	32,57
	2-butanone (methyl ethyl ketone)	Water	25	100	28.4	38.4	−0.38	−3.2	−3.7	−38.5	−40.2	1.6	LCST = −6°C UCST = 150°C	32,57
	n-heptanol	Water ($T < 50$°C)	25	50	3760	4765	−0.35	−7.2	–	−92.6	–	3.8		32,57
	Triethylamine	Water					Candidate for further study.						LCST = 19°C	32,57
	Nicotine	Water					Candidate for further study.						LCST = 61°C	32,57
	Ethylbenzylamine	1,2,3-trihydroxypropane (glycerol)					Candidate for further study.						LCST	91
	2-methoxy phenol (guaiacol)	1,2,3-trihydroxypropane (+ 2.2% water by volume)					Candidate for further study.						LCST = 56°C UCST = 69°C	91,97
	3-methylaniline (*m*-toluidine)	1,2,3-trihydroxypropane					Candidate for further study.						LCST	100
V	Net Attractive Interactions with Negative Excess Entropy						Pos.	Neg.		Neg.		Pos.		
	2-propanone (acetone)	Trichloromethane (chloroform)	32	50	0.39	0.48	4.3	−11.2[a]	−7.7[a]	−28.9[a]	−17.8[a]	0.77	CM	70
	1,4-dioxane	[BMPYR][TCM][c]	45	95	0.642	0.768	3.6	−4.9[a]	−3.7	−11.8[a]	−8.0	0.72	CM	94
	trichloromethane	Ethyl acetate	37	76	0.424	0.512	2.1	−4.8[a]	−4.3	−8.5	−6.7	0.52	CM	55
	Tetrahydrofuran	Trichloromethane	32	50	0.21	0.25	2.1	−8.37[a]	−7.44	−14.5[a]	−11.5	0.52	CM	70
	Pyridine	[BMPYR][TCM][c]	45	95	0.567	0.627	1.3	−2.05[a]	−1.98	−1.73[a]	−1.49	0.25	CM	94
	Trichloromethane	2-propanone	34	56	0.503	0.530	1.1	−2.02[a]	−1.98[a]	−0.85[a]	−0.75[a]	0.12	CM	55
VI	Net Attractive Interactions with Positive Excess Entropy						Pos.	Neg.		Pos.		Neg.		
	Methanol	*N*-methylpyrrolidone	60	90	0.482	0.511	0.97	−1.95[a]	−1.96	0.22[a]	0.20	−0.03	CM	90
	Benzene	[3C6C14P][BTI][d]	40	100	0.391	0.437	0.72	−1.73[a]	−1.79	2.27[a]	2.1	−0.39	CM	101
	2-propanone (acetone)	[3C6C14P][BTI][d]	40	100	0.297	0.334	0.58	−1.80[a]	−1.88	4.36[a]	4.09	−0.72	CM	101
	Ethanol	*N*-methylpyrrolidone	60	90	0.606	0.618	0.46	−0.61[a]	−0.64	2.35[a]	2.24	−1.17	CM	90
VII	Chemically Similar, Wide Molecular Size Distribution						Neg.	Pos.		Pos.		Pos.		
	Methanol	[BMPYR][TCM][c]	45	95	0.699	0.590	−2.7	1.98[a]	2.98	9.16[a]	12.3	1.37	CM	94
	Hexane	C_{36}	76	88	0.640	0.628	−1.2	1.12[a]	1.43[a]	6.8[a]	7.8[a]	1.81	CM	102
	Nonane	C_{36}	76	88	0.727	0.717	−1.3	0.82[a]	1.43[a]	4.9[a]	7.8[a]	1.79	CM	102
	Heptane	C_{16}	20	50	0.924	0.921	−0.41	0.08	0.10[a]	0.94	0.98[a]	3.44	CM	102

[a]Extrapolated value. All other values are determined by interpolation between temperatures T_{low} and T_{high}.
[b]Completely miscible, but near a phase instability condition.
[c]1-butyl-1-methylpyrrolidinium tricyanomethanide (ionic liquid).
[d]Trihexyltetradecylphosphonium bis (trifluoromethylsulfonyl) imide (ionic liquid).
[e]Type III includes alcohols in water (C_8 and above). It also includes C_4–C_7 alcohols in water at $T > 50$°C.
[f]Type IV includes C_4–C_7 alcohols in water at $T < 50$°C.

Table 4. Average θ for Nonaqueous Solute–Solvent Pairings (Types II and III)

Solute Class	Solvent Class	θ	No. of Datasets	Relative Error (%)
Active Hydrogen	Active Hydrogen	2.8	11	25.6
Active Hydrogen	Aromatic	2.1	6	15.6
Active Hydrogen	Nonpolar	2.8	33	24.2
Active Hydrogen	Polar	1.8	35	16.8
Aromatic	Active Hydrogen	0.6	22	19.0
Aromatic	Aromatic	1.4	10	12.5
Aromatic	Nonpolar	2.4	8	8.4
Aromatic	Polar	1.5	32	15.3
Nonpolar	Active Hydrogen	0.7	53	12.4
Nonpolar	Aromatic	1.6	34	14.7
Nonpolar	Polar	1.4	106	18.8
Polar	Active Hydrogen	2.1	63	20.7
Polar	Aromatic	2.8	15	21.7
Polar	Nonpolar	2.3	64	15.4
Polar	Polar	1.4	76	15.0

Type VII. Chemically similar, wide molecular size distribution

Type VII binaries are completely miscible. Excess entropy is positive and excess enthalpy effects are relatively small and positive, so the activity coefficient is less than but close to unity (Table 3). Our analysis of the limited data available for this type indicates that θ_{ij} falls in the range of $-5 < \theta_{ij} < -0.5$. For this type of mixture, the entropic contribution to γ_{ij}^{∞} dominates. It is approximated by the classic Flory–Huggins equation written for chemically similar components[102]

$$\ln \gamma_{ij}^{\infty}(\text{entropic}) = \ln\left(\frac{V_i^L}{V_j^L}\right) + 1 - \frac{V_i^L}{V_j^L} \tag{11}$$

where the effect of temperature is in the temperature dependence of molar volumes V_i^L and V_j^L. Kato et al.[102] studied literature data for binary mixtures of C_4–C_{10} hydrocarbons dissolved in C_{12}–C_{36} hydrocarbons for which $0.6 < \gamma_{ij}^{\infty} < 1$ and γ_{ij}^{∞} tends to decrease slightly with increasing temperature. The authors concluded that both $\overline{h}_{ij}^{E,\infty}$ and $\overline{s}_{ij}^{E,\infty}$ must be positive, and they evaluated various activity coefficient models including Eq. 11. Another binary of this type is methanol dissolved in the ionic liquid [BMPYR][TCM] for which γ_{ij}^{∞} is on the order of 0.6 to 0.7 and decreases with increasing temperature.[94] Both solute and solvent are polar and $\overline{h}_{ij}^{E,\infty}$ is small relative to $T\overline{s}_{ij}^{E,\infty}$, so the large size difference appears to be the main factor affecting γ_{ij}^{∞} (Table 3).

Applications

The proposed method can be used with current methods used for correlating or extrapolating limiting activity coefficients as a function of composition. One such method[114] involves extrapolation of γ_{ij}^{∞} from a given solvent j to a new

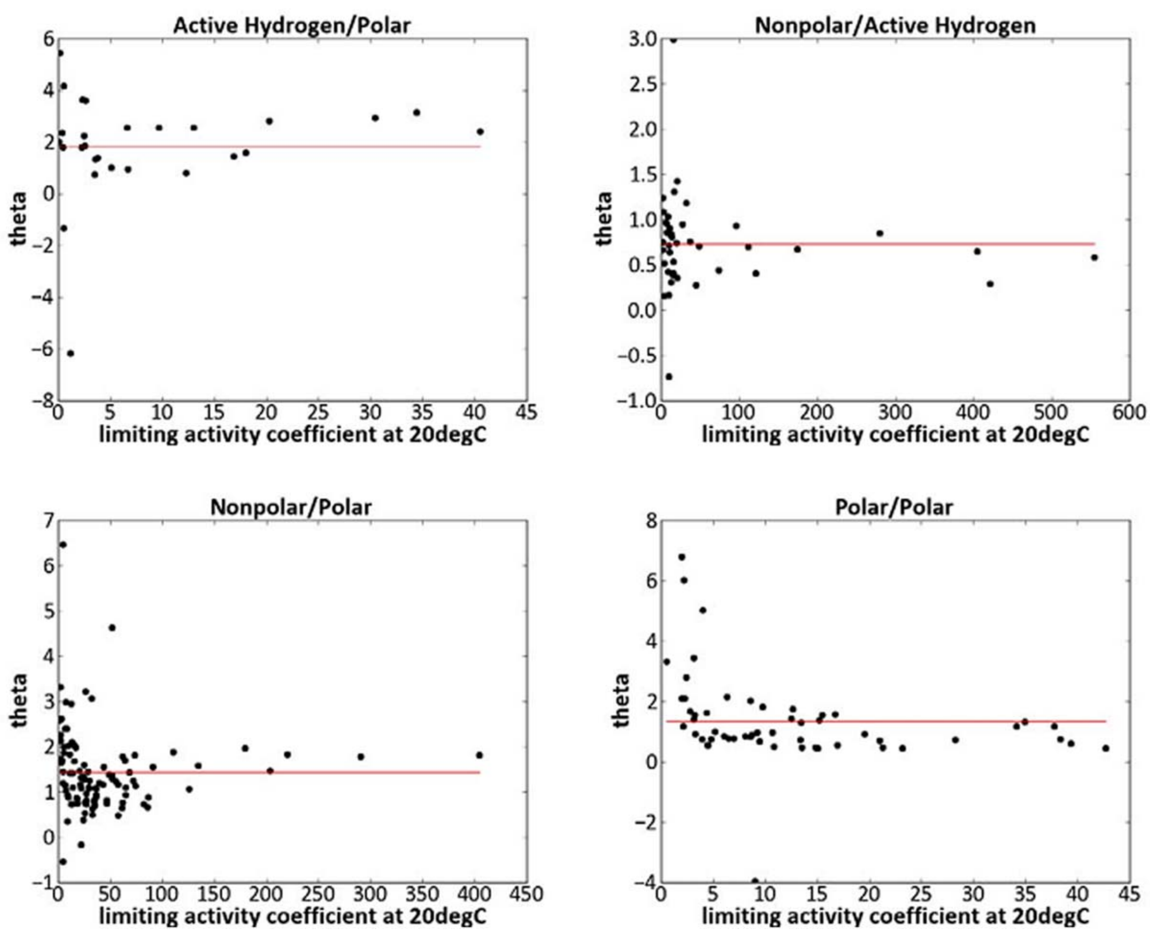

Figure 5. Temperature dependence parameter θ_{ij} plotted vs. γ_{ij}^{∞} data at 20°C for general pairings of solute and solvent (Types II and III).

[Color figure can be viewed in the online issue, which is available at wileyonlinelibrary.com.]

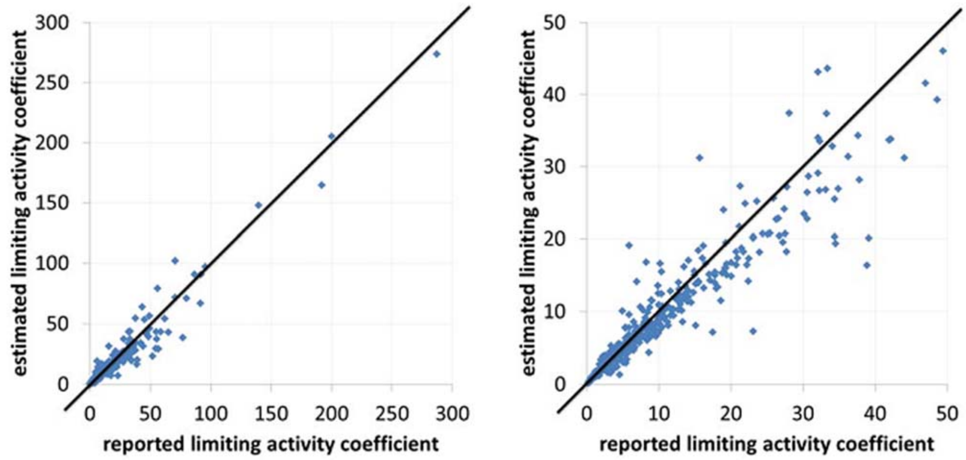

Figure 6. Estimated γ_{ij}^{∞} vs. experimental data.

Estimates were obtained using Eq. 1 and values of θ listed in Table 4 for general kinds of solute–solvent pairings (Types II and III). [Color figure can be viewed in the online issue, which is available at wileyonlinelibrary.com.]

solvent k as a means to calculating the activity coefficient for solute i dissolved in a variety of solvents. Application of Eq. 1 using an estimate of θ_{ik} for the new solute–solvent pairs allows extrapolation as a function of temperature. Table 5 summarizes various applications in separation process analysis and environmental studies where a form of Eq. 1 is easily inserted into the analysis.

The parameter θ_{ij} also can be incorporated directly into an excess Gibbs energy expression. It is a common practice to represent the effect of temperature for a given binary interaction parameter using empirical expressions with 2 or more correlation constants.[3,5,119,122–124] This is a common option offered by commercially available process simulation software.[124] Typical expressions have the form $\ln A$ or $A = a + b/T + c\ln T$ where A is a model parameter and a, b, and c are correlation constants determined by fitting data. We propose simplifying this approach by instead expressing the temperature dependence in terms of θ_{ij}.

For example, for a binary mixture a modified version of the van Laar correlation has the form

$$\ln \gamma_i = \frac{a_{ij}\left(T_{\mathrm{ref}}/T\right)^{\theta_{ij}}}{\left(1+\frac{a_{ij}x_i}{a_{ji}x_j}\right)^2} \tag{12}$$

$$\ln \gamma_j = \frac{a_{ji}\left(T_{\mathrm{ref}}/T\right)^{\theta_{ji}}}{\left(1+\frac{a_{ji}x_j}{a_{ij}x_i}\right)^2} \tag{13}$$

where x_i and x_j are liquid-phase mole fractions, and the correlation constants are given by $a_{ij} = \ln \gamma_{ij}^{\infty}$ at $T = T_{\mathrm{ref}}$, $a_{ji} = \ln \gamma_{ji}^{\infty}$ at $T = T_{\mathrm{ref}}$, as in Eq. 1. An application is shown in Figure 7 for the 2-propanone + ethanol system (Type II). Poor fit of activity coefficients at dilute conditions is a well-known limitation of the classic van Laar equations; however, in this example the modified van Laar equations gave much improved representation of γ_{ij}^{∞} (Figure 7) while retaining good representation of γ_i for correlating vapor–liquid equilibrium data at more concentrated conditions (not shown). This improvement results from the introduction of an entropic term as indicated by Eq. 9.

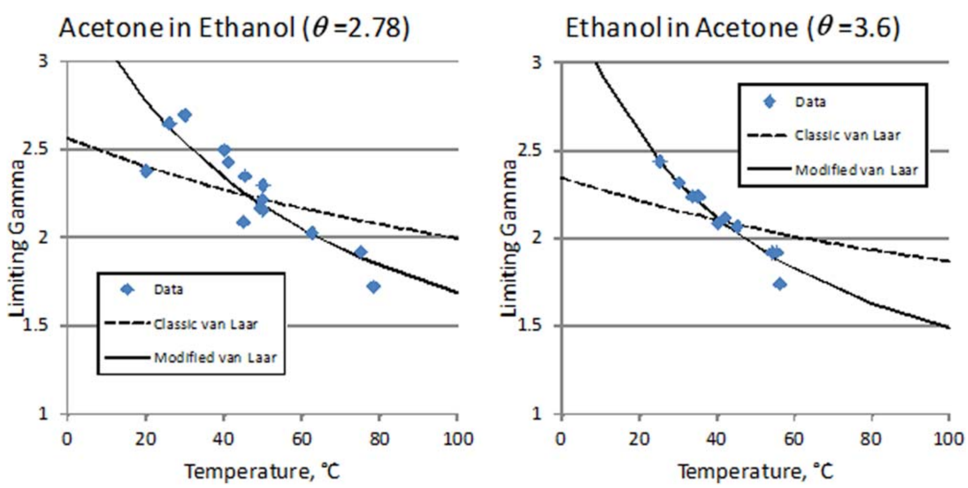

Figure 7. Application of the modified van Laar correlation to 2-propanone (acetone) + ethanol (Type II).

For the modified van Laar correlation (Eqs. 12 and 13), $\theta_{ij} = 2.78$, $\theta_{ji} = 3.60$, and $a_{ij} = 0.977$, $a_{ji} = 0.876$ at $T_{\mathrm{ref}} = 298$ K. For the classic van Laar correlation, $\theta_{ij} = \theta_{ji} = 1.0$, and $a_{ij} = 0.863$, $a_{ji} = 0.780$ at $T_{\mathrm{ref}} = 298$ K. In the classic case ($\theta = 1$), $a_{ij} = A/RT_{\mathrm{ref}}$ and $a_{ji} = B/RT_{\mathrm{ref}}$, where A and B are the standard van Laar correlation constants defined in Ref. 5, Table 8-3. Data were taken from the following references:[55,65,70,103–106]. [Color figure can be viewed in the online issue, which is available at wileyonlinelibrary.com.]

Table 5. Equations for Process Separations and Environmental Studies

Application	Key Equations Modified by Using Eq. 1	Background References[a]
Screening solvents for extractive distillation and entrainers for azeotropic distillation	relative volatility, $\alpha_{ik}^{\infty}\big\vert_{\text{in a solvent or entrainer}} = \frac{\gamma_{i,\text{solvent}}^{\infty}(T)}{\gamma_{k,\text{solvent}}^{\infty}(T)} \frac{p_i^{\text{SAT}}(T)}{p_k^{\text{SAT}}(T)} = \frac{\exp\left[\ln\gamma_{i,\text{solvent}}^{\infty}(\text{at } T_{\text{ref}})\times(T_{\text{ref}}/T)^{\theta_{i,\text{solvent}}}\right]}{\exp\left[\ln\gamma_{k,\text{solvent}}^{\infty}(\text{at } T_{\text{ref}})\times(T_{\text{ref}}/T)^{\theta_{k,\text{solvent}}}\right]} \frac{p_i^{\text{SAT}}(T)}{p_k^{\text{SAT}}(T)}$	9,115
Stripping mode distillation at dilute solute conditions	$\alpha_{ij}^{\infty} = \gamma_{ij}^{\infty}(T)\frac{p_i^{\text{SAT}}(T)}{p_j^{\text{SAT}}(T)} = \exp\left[\ln\gamma_{ij}^{\infty}(\text{at } T_{\text{ref}})\times(T_{\text{ref}}/T)^{\theta_{ij}}\right]\frac{p_i^{\text{SAT}}(T)}{p_j^{\text{SAT}}(T)}$	9,99,115, 116
Screening solvents for liquid-liquid extraction at dilute conditions	partition ratio, K_i^{∞} $K_i^{\infty} = \frac{x_i^{\text{extract}}}{x_i^{\text{raffinate}}} = \frac{\gamma_{i,\ \text{raffinate}}^{\infty}(T)}{\gamma_{i,\ \text{extract}}^{\infty}(T)} = \frac{\exp\left[\ln\gamma_{i,\text{raffinate}}^{\infty}(\text{at } T_{\text{ref}})\times(T_{\text{ref}}/T)^{\theta_{i,\text{raffinate}}}\right]}{\exp\left[\ln\gamma_{i,\text{extract}}^{\infty}(\text{at } T_{\text{ref}})\times(T_{\text{ref}}/T)^{\theta_{i,\text{extract}}}\right]}$	9,10,99
Henry's Law constants for organics dissolved in water	Henry's Law constant, $H_i = \gamma_{i,\text{water}}^{\infty}(T)\frac{p_i^{\text{SAT}}(T)}{\rho_{\text{water}}(T)} = \exp\left[\ln\gamma_{i,\text{water}}^{\infty}(\text{at } T_{\text{ref}})\times(T_{\text{ref}}/T)^{\theta_{i,\text{water}}}\right]\frac{p_i^{\text{SAT}}(T)}{\rho_{\text{water}}(T)}$	95,96,117–119
Octanol-water partition coefficients at dilute conditions	$K_{\text{ow},i}^{\infty} \equiv \frac{x_i^{\text{octanol-rich phase}}}{x_i^{\text{aqueous phase}}}\frac{\rho_{\text{octanol-rich phase}}}{\rho_{\text{aqueous phase}}} = \frac{\gamma_{i,\text{water + dissolved octanol}}^{\infty}}{\gamma_{i,\text{octanol + dissolved water}}^{\infty}}\frac{\rho_{\text{octanol-rich phase}}}{\rho_{\text{aqueous phase}}} \approx \frac{\gamma_{i,\text{water}}^{\infty}(T)}{\gamma_{i,\text{organic phase}}^{\infty}(T)}\frac{\rho_{\text{organic phase}}(T)}{\rho_{\text{water}}(T)} = \frac{\exp\left[\ln\gamma_{i,\text{water}}^{\infty}(\text{at } T_{\text{ref}})\times(T_{\text{ref}}/T)^{\theta_{i,\text{water}}}\right]}{\exp\left[\ln\gamma_{i,\text{organic phase}}^{\infty}(\text{at } T_{\text{ref}})\times(T_{\text{ref}}/T)^{\theta_{i,\text{organic phase}}}\right]}\frac{\rho_{\text{organic phase}}(T)}{\rho_{\text{water}}(T)}$	117,120,121

[a]See background references for detailed discussion of the standard nomenclature: $\alpha_{i,k}$ is the relative volatility of component i with respect to k, K_i^{∞} is the liquid-liquid partition ratio at dilute solute concentrations, $K_{\text{ow},i}^{\infty}$ is the octanol-water partition coefficient for solute i, p_i^{SAT} is pure component vapor pressure, x_i is mole fraction concentration in the liquid, and ρ is liquid molar density.

Equation 1 also can be used to modify the extended Hansen model,[12] as follows

$$\ln\gamma_{ij}^{\infty} = a_{ij}(T_{\text{ref}}/T)^{\theta_{ij}} = \frac{V_i^L(T_{\text{ref}}/T)^{\theta_{ij}}}{RT_{\text{ref}}} \times\left\{\left(\delta_i^d-\delta_j^d\right)^2+0.25\left[\left(\delta_i^p-\delta_j^p\right)^2+\left(\delta_i^h-\delta_j^h\right)^2\right]\right\} \tag{14}$$

where δ^d, δ^p, and δ^h are the pure-component Hansen solubility parameters[12,14,39] obtained at some reference temperature T_{ref} (normally room temperature). Mixed solvents and concentrations away from infinite dilution are evaluated using average molar-volume weighted δ values.[12] Only Types I–IV are applicable in this case, as Eq. 14 is unable to represent $\gamma_{ij}^{\infty} < 1$.

For the Wilson and NRTL correlations,[3,5] the temperature dependence can be modeled by inserting Eq. 1 into their respective equations for $\ln\gamma_{ij}^{\infty}$. For the Wilson equation written using the standard nomenclature, this yields

$$\ln\gamma_{ij}^{\infty} = a_{ij}(T_{\text{ref}}/T)^{\theta_{ij}} = 1-\ln\Lambda_{ij}-\Lambda_{ji} \tag{15}$$

where Λ_{ij} and Λ_{ji} are model parameters and $a_{ij}=\ln\gamma_{ij}^{\infty}$ at $T=T_{\text{ref}}$, $a_{ji}=\ln\gamma_{ji}^{\infty}$ at $T=T_{\text{ref}}$. Instead of using the functional form $\Lambda_{ij}=V_j^L/V_i^L\exp\left(-\lambda_{ij}/RT\right)$ from the original model, values of Λ_{ij} and Λ_{ji} can be obtained as a function of temperature by simultaneously solving the equations

$$\Lambda_{ij} = 1-a_{ji}(T_{\text{ref}}/T)^{\theta_{ji}}-\ln\Lambda_{ji} \tag{16}$$

$$\Lambda_{ji} = 1-a_{ij}(T_{\text{ref}}/T)^{\theta_{ij}}-\ln\Lambda_{ij} \tag{17}$$

Parameter values corresponding to specific temperatures can be adjusted as needed to optimize the data fit across the entire composition range. Similarly, for the NRTL equations[3] we obtain

$$\ln\gamma_{ij}^{\infty} = a_{ij}(T_{\text{ref}}/T)^{\theta_{ij}} = \tau_{ij}\exp\left(-\alpha_{ij}\tau_{ij}\right)+\tau_{ji} \tag{18}$$

$$\tau_{ij} = a_{ji}(T_{\text{ref}}/T)^{\theta_{ji}}-\tau_{ji}\exp\left(-\alpha_{ji}\tau_{ji}\right) \tag{19}$$

$$\tau_{ji} = a_{ij}(T_{\text{ref}}/T)^{\theta_{ij}}-\tau_{ij}\exp\left(-\alpha_{ij}\tau_{ij}\right) \tag{20}$$

where τ_{ij} and τ_{ji} are the temperature-dependent model parameters, and α_{ij} and α_{ji} are model parameters assumed to be independent of temperature.

In principle, this general approach may be applied to other excess Gibbs energy expressions, as well. Suitable θ_{ij} values may be estimated via Eq. 9 or treated as adjustable model parameters in fitting data. Estimates also may be obtained from molecular structure for specific classes of compounds, as summarized in Table 4. The range of possible θ_{ij} values is bounded by the range of values given in Tables 2–4 for a given binary type—for applications within the normal temperature range.

Summary

We have introduced a new temperature-dependence parameter θ_{ij} and a systematic classification scheme for correlating infinite-dilution activity coefficients of nonionic organic solutes. Many different types of temperature dependence are possible depending on the signs and relative magnitudes of partial molar excess enthalpy and entropy, and we have shown that θ_{ij} can be related to these basic thermodynamic properties such that $\theta_{ij}=1/[1-(T\bar{s}_{ij}^{E,\infty}/\bar{h}_{ij}^{E,\infty})]$. We have also provided examples where a constant value of θ_{ij} allows correlation of $\gamma_{ij}^{\infty}=f(T)$ over a reasonably wide temperature span. Exceptions include a number of organic + water binaries.

To provide a framework for organizing data, we have classified solute–solvent binary pairs into seven types corresponding to distinct domains of γ_{ij}^{∞} and θ_{ij} (Tables 1 and 2). Table 3 lists values of θ_{ij} for representative binaries determined by regression of temperature-dependent γ_{ij}^{∞} data. This table can readily be expanded to include additional temperature-dependent data available in the literature. In principle, when data are lacking, estimates of θ_{ij} may be obtained using methods aimed at calculating relative values of $\overline{h}_{ij}^{E,\infty}$ and $\overline{s}_{ij}^{E,\infty}$. For nonaqueous binaries containing specific classes of compounds, estimates may be obtained from molecular structure using the method summarized in Table 4. The resulting framework should be useful for application-directed screening and modeling purposes, as illustrated by Table 5 and Eqs. 12–20.

Acknowledgments

We gratefully acknowledge valuable discussions with Professor Charles Eckert of Georgia Institute of Technology. We have greatly benefited from his work and insights. We also thank Felipe Donate, Sumnesh Gupta, James Olson, Lanny Robbins, and Rakesh Srivastava for valuable discussions, and the management of The Dow Chemical Company for their support.

Literature Cited

1. Berg C, McKinnis, AC. Effect of temperature on liquid phase activity coefficients. *Ind Eng Chem.* 1948;40(7):1309–1311.
2. Pierotti GJ, Deal CH, Derr EL. Activity coefficients and molecular structure. *Ind Eng Chem.* 1959;51(1):95–102.
3. Walas SM. *Phase Equilibria in Chemical Engineering*. Butterworth-Heinemann: Boston, 1985.
4. Prausnitz JM, Lichtenthaler RN, Gomes de Azevedo E. *Molecular Thermodynamics of Fluid-Phase Equilibria, 3rd ed.* Prentice Hall PTR: Upper Saddle River, New Jersey, 1999.
5. Poling BE, Prausnitz JM, O'Connell JP. *The Properties of Gases and Liquids, 5th ed.* McGraw-Hill: New York, 2001.
6. Sandler SI. *Chemical, Biochemical, and Engineering Thermodynamics, 4th ed.* Wiley: Hoboken, New Jersey, 2006.
7. Elliot JR, Lira CT. *Introductory Chemical Engineering Thermodynamics, 2nd ed.* Prentice Hall PTR: Upper Saddle River, New Jersey, 2012.
8. O'Connell JP, Haile JM. *Thermodynamics. Fundamentals for Applications.* Cambridge University Press: Cambridge, 2005.
9. Rousseau RW, editor. *Handbook of Separations Process Technology.* Wiley-Interscience: New York, 1987.
10. Frank TC, Dahuron L, Holden BS, Prince WD, Seibert AF, Wilson LC. Liquid-liquid extraction and other liquid-liquid operations and equipment. In: Section 15 in Green DW, editor. *Perry's Chemical Engineers' Handbook, 8th ed.* McGraw-Hill: New York, 2007.
11. Frank TC, Anderson JJ, Olson JM, Eckert CA. Application of MOSCED and UNIFAC to screen hydrophobic organic solvents for extraction of hydrogen-bonding organics from aqueous solution. *Ind Eng Chem Res.* 2007;46(13):4621–4625.
12. Frank TC, Downey JR, Gupta SK. Quickly screen solvents for organic solids. *Chem Eng Prog.* 1999;95(12):41–61.
13. Kolář P, Shen J-W, Tsuboi A, Ishikawa T. Solvent selection for pharmaceuticals. *Fluid Phase Equilib.* 2002;194–197:771–782.
14. Barton AFM. *Handbook of Solubility Parameters and Other Cohesion Parameters, 2nd ed.* CRC Press: Boca Raton, Florida, 1991.
15. Johansson I, Somasundaran P, editors. *Handbook of Cleaning/Decontamination of Surfaces.* Elsevier: Amsterdam, 2007.
16. Chen L-J, Lin S-Y, Chern C-S, Wu S-C. Critical micelle concentration of mixed surfactant SDS/NP(EO)40 and its role in emulsion polymerization. *Colloids Surf A.* 1997;122:161–168.
17. Piccoli RL, Lovisi HR. Kinetic and thermodynamic study of the liquid-phase etherification of isoamylenes with methanol. *Ind Eng Chem Res.* 1995;34(2):510–515.
18. Vitha M, Carr PW. The chemical interpretation and practice of linear solvation energy relationships in chromatography. *J Chromatogr A.* 2006;1126:143–194.
19. Fitts CR. *Groundwater Science.* Academic Press: London, 2002.
20. Kontogeorgis GM, Folas GK. *Thermodynamic Models for Industrial Applications.* Wiley: Chichester, UK, 2010.
21. Schreiber LB, Eckert CA. Use of infinite dilution activity coefficients with Wilson's equation. *Ind Eng Chem Proc Des Dev.* 1971; 10(4):572–576.
22. Gmehling J, Kolbe B. Limitations of modern expressions for the excess Gibbs energy. *Fluid Phase Equilib.* 1983;13:227–242.
23. Prausnitz JM, Tavares FW. Thermodynamics of fluid-phase equilibria for standard chemical engineering operations. *AIChE J.* 2004; 50(4):739–761.
24. Gupta S, Olson JD. Industrial needs in physical properties. *Ind Eng Chem Res.* 2003;42(25):6359–6374.
25. Robbins LA. Liquid-liquid extraction: a pretreatment process for wastewater. *Chem Eng Prog.* 1980;76(10):58–61.
26. Godfrey NB. Solvent selection via miscibility number. *Chemtech.* 1972;2(6):359–363.
27. Padovani AM, Suleiman D. Simple prediction of limiting activity coefficients of nonelectrolytes in water at 25°C. *AIChE J.* 1997; 43(12):3271–3273.
28. Jakob A, Grensemann H, Lohmann J, Gmehling J. Further development of modified UNIFAC (Dortmund): revision and extension 5. *Ind Eng Chem Res.* 2006;45(23):7924−7933.
29. Gmehling J. Potential of group contribution methods for the prediction of phase equilibria and excess properties of complex mixtures. *Pure Appl Chem.* 2003;75(7):875–888.
30. Weidlich U, Gmehling J. A modified UNIFAC model. 1. Prediction of VLE, hE, and γi. *Ind Eng Chem Res.* 1987;26(7):1372–1381.
31. Thomas ER, Eckert CA. Prediction of limiting activity coefficients by a modified separation of cohesive energy density model and UNIFAC. *Ind Eng Chem Proc Des Dev.* 1984;23(2):194–209.
32. Lazzaroni MJ, Bush D, Eckert CA, Frank TC, Gupta SK, Olson JD. Revision of MOSCED parameters and extension to solid solubility calculations. *Ind Eng Chem Res.* 2005;44(11):4075–4083; plus Supporting Information (database of published limiting activity coefficients).
33. Klamt A, Eckert F, Arlt W. COSMO-RS: an alternative to simulation for calculating thermodynamic properties of liquid mixtures. *Annu Rev Chem Biomole Eng.* 2010;1:101–122.
34. Mullins E, Oldland R, Liu YA, Wang S, Sandler SI, Chen C-C, Zwolak M, Seavey KC. Sigma-profile database for using COSMO-based thermodynamic methods. *Ind Eng Chem Res.* 2006;45(12): 4389–4415.
35. Hsieh C-M, Sandler SI, Lin S-T. Improvements of COSMO-SAC for vapor-liquid and liquid-liquid equilibrium predictions. *Fluid Phase Equilib.* 2010;297:90–97.
36. Chen C-C, Song Y. Solubility modeling with a nonrandom two-liquid segment activity coefficient model. *Ind Eng Chem Res.* 2004; 43(26):8354−8362.
37. Possani LFK, Flôres GB, Staudt PB, Soares R de P. Simultaneous correlation of infinite dilution activity coefficient, vapor-liquid, and liquid-liquid equilibrium data with F-SAC. *Fluid Phase Equilib.* 2014;364:31–41.
38. Hait MJ, Liotta CL, Eckert CA, Bergmann DL, Karachewski AM, Dallas AJ, Eikens DI, Li JJ, Carr PW, Poe RB, Rutan SC. SPACE predictor for infinite dilution activity coefficients. *Ind Eng Chem Res.* 1993;32(11):2905–2914.
39. Hansen CM. *Hansen Solubility Parameters: A User's Handbook, 2nd ed.* CRC Press: Boca Raton, Florida, 2007.
40. Sherman SR, Suleiman D, Hait MJ, Schiller M, Liotta CL, Eckert CA, Li J, Carr PW, Poe RB, Rutan SC. Correlation of partial molar heats of transfer at infinite dilution by a linear solvation energy relationship. *J Phys Chem.* 1995;99(28):11239–11247.
41. Orbey H, Sandler SI. On the combination of equation of state and excess free energy models. *Fluid Phase Equilib.* 1995;111:53–70.
42. Kontogeorgis GM, Coutsikos P. Thirty years with EoS/GE models—what have we learned? *Ind Eng Chem Res.* 2012;51:4119–4142.
43. Kaptay G. A new equation for the temperature dependence of the excess Gibbs energy of solution phases. *CALPHAD.* 2004;28(2): 115–124.
44. Kaptay G. On the abilities and limitations of the linear, exponential, and combined models to describe the temperature dependence of the excess Gibbs energy of solutions. *CALPHAD.* 2014;44:81–94.
45. Reinisch J, Klamt A, Eckert F, Diedenhofen M. Prediction of the temperature dependence of a polyether-water mixture using COSMOtherm. *Fluid Phase Equilib.* 2011;310:7–10.
46. Klamt A, Reinisch J, Eckert F, Graton J, Le Questel J-Y. Interpretation of experimental hydrogen-bond enthalpies and entropies from

COSMO polarisation charge densities. *Phys Chem Chem Phys.* 2013; 15:7147–7154.
47. Maginn EJ, Elliott JR. Historical perspective and current outlook for molecular dynamics as a chemical engineering tool. *Ind Eng Chem Res.* 2010;49:3059–3078.
48. Dowdle JR, Buldyrev SV, Stanley HE, Debenedetti PG, Rossky PJ. Temperature and length scale dependence of solvophobic solvation in a single-site water-like liquid. *J Chem Phys.* 2013;138(064506):1–12.
49. dos Ramos MC, Páez AV, Piñeiro MM, Blas FJ. An examination of the excess thermodynamic properties of flexible molecules from a molecular modeling perspective. *Fluid Phase Equilib.* 2014;361:93–103.
50. Umer M, Albers K, Sadowski G, Leonard K. PC-SAFT parameters from ab initio calculations. *Fluid Phase Equilib.* 2014;362:41–50.
51. Wyczalkowski MA, Vitalis A, Pappu RV. New estimators for calculating solvation entropy and enthalpy and comparative assessments of their accuracy and precision. *J Phys Chem.* 2010;114(24):8166–8180.
52. Carlsson J, Aaqvist J. Calculations of solute and solvent entropies from molecular dynamics simulations. *J Chem Chem Phys.* 2006; 8(46):5385–5395.
53. Sarkar S, Bagchi B. Inherent structures of phase-separating binary mixtures: nucleation, spinodal decomposition, and pattern formation. *Phys Rev E.* 2011;83(3 Pt 1):031506.
54. Tessier SR, Brennecke JF, Stadtherr MA. Reliable phase stability analysis for excess Gibbs energy models. *Chem Eng Sci.* 2000; 55(10):1785–1796.
55. Trampe DM, Eckert CA. Limiting activity coefficients from an improved differential boiling point technique. *J Chem Eng Data.* 1990;35(2):156–162.
56. Atik Z, Gruber D, Krummen K, Gmehling J. Measurement of activity coefficients at infinite dilution of benzene, toluene, ethanol, esters, ketones, and ethers at various temperatures in water using the dilutor technique. *J Chem Eng Data.* 2004;49:1429–1432.
57. Onken U, Rarey-Nies J, Gmehling J. The Dortmund data bank: a computerized system for retrieval, correlation, and prediction of thermodynamic properties of mixtures. *Int J Thermophys.* 1989;10(3): 739–747. The latest data bank is available from DDBST GmbH at http://www.ddbst.com. Last accessed March 5, 2014.
58. Christensen JJ, Hanks RW, Izatt RM. *Handbook of Heats of Mixing*. Wiley: New York, 1982.
59. Christensen JJ, Rowley RL, Izatt RM, *Handbook of Heats of Mixing*. Supplemental Volume, Wiley: New York, 1988.
60. Mueller CR, Kearns ER. Thermodynamic studies of the system acetone and chloroform. *J Phys Chem.* 1958;62:1441–1445.
61. Hovorka S, Dohnal V, Roux AH, Roux-Desgranges G. Determination of temperature dependence of limiting activity coefficients for a group of moderately hydrophobic organic solutes in water. *Fluid Phase Equilib.* 2002;201:135–164.
62. Silverstein TP. The real reason why oil and water don't mix. *J Chem Ed.* 1998;75(1):116–118.
63. Soper AK, Dougan L, Crain J, Finney JL. Excess entropy in alcohol-water solutions: a simple clustering explanation. *J Phys Chem B.* 2006;110(8):3472–3476.
64. Han S-J. New types of inclined ebulliometers for the determination of activity coefficients at infinite dilution. *Int Chem Eng.* 1991;31(1): 171–177.
65. Dallinga L, Schiller M, Gmehling J. Measurement of activity coefficients at infinite dilution using differential ebulliometry and nonsteady-state gas-liquid chromatography. *J Chem Eng Data.* 1993; 38(1):147–155.
66. Bao J-B, Hang -L, Han S-J. Infinite-dilution activity coefficients of (propanone + an n-alkane) by gas stripping. *J Chem Thermodyn.* 1994;26:673–680.
67. Deal CH, Derr EL. Selectivity and solvency in aromatics recovery. *Ind Eng Chem Proc Des Dev.* 1964;3:394–399.
68. Magiera B, Brostow W. Vapor-liquid equilibria of binary mixtures of carbon-14 labeled hexane with aliphatic ketones. *J Phys Chem.* 1971;74:4041–4047.
69. Dohnal V, Horáková I. A new variant of the Rayleigh distillation method for the determination of limiting activity coefficients. *Fluid Phase Equilib.* 1991;68:173–185.
70. Thomas ER, Newman BA, Long TC, Wood DA, Eckert CA. Limiting activity coefficients of nonpolar and polar solutes in both volatile and nonvolatile solvents by gas chromatography. *J Chem Eng Data.* 1982;27(4):399–405.
71. Lafyatis DS, Scott LS, Trampe DM, Eckert CA. A test of the functional dependence of gE(x) liquid-liquid equilibria using limiting activity coefficients. *Ind Eng Chem Res.* 1989;28(5):585–590.
72. Nikolić AD, Perišić-Janjić NU. A thermodynamic study of N-n-butylbenzamide solutions using gas-liquid chromatography. *J Chem Thermodyn.* 1985;17(9):849–853.
73. Castells CB, Eikens DI, Carr PW. Headspace gas chromatographic measurements of limiting activity coefficients of eleven alkanes in organic solvents at 25°C. *J Chem Eng Data.* 2000;45(2):369–375.
74. Alessi P, Kikic I, Tlustos G. Activity coefficients of hydrocarbons in glycols. *Chim Ind.* 1971;53(10):925–928.
75. Alessi P, Kikic I, Torriano G. Activity coefficients of hydrocarbons in phthalates. *J Chromatogr A.* 1975;105(2):257–264.
76. Arancibia EL, Catoggio JA. Gas chromatographic study of solution and adsorption of hydrocarbons on glycols: I. Diethylene glycol and triethylene glycol. *J Chromatogr A.* 1980;197(2):135–145.
77. Endler I, Hradetzky G, Bittrich HJ. Borderline activity-coefficients of hydrocarbons in diethylene glycol with kinetic drag methods. *Z Phys Chem.* 1984;265:409–411.
78. Vernier P, Rairnbault C, Renon HJ. Activity coefficients of hexane in 4-methyl-1,3-dioxolan-2-one. *Chim Phys.* 1969;66(5):960.
79. Gaile AA, Parizheva NV, Proskuryakov VA. Selectivity and solvent power of extractants for aromatic hydrocarbons. *Zh Prikl Khim.* 1974;47(l):191.
80. Sarius A, Lempe D, Bittrich HJ. Untersuchungen zur selektiven stofftrennung. *Chem Technol.* 1978;30:585.
81. Zakharov AP, Gaile AA, Proskuryakov VA, Te LB. Selectivity of lactones with respect to the hexane-benzene system. *Zh Fiz Khim.* 1978;52(6):1479–1482.
82. Dixit S, Crain J, Poon WCK, Finney JL, Soper AK. Molecular segregation observed in a concentrated alcohol-water solution. *Nature.* 2002;416:829–832.
83. Leff HS. Entropy, its language, and interpretation. *Found Phys.* 2007;37:1744–1766.
84. Lambert FL. The conceptual meaning of thermodynamic entropy in the 21st century. *Int Res J Pure Appl Chem.* 2011;1(3):65–68.
85. Lambert FL, Leff HS. The correlation of standard entropy with enthalpy supplied from 0 to 298.15 K. *J Chem Ed.* 2009;86(1):94–98.
86. Grant DJW, Higuchi T. *Solubility Behavior of Organic Compounds. Techniques of Chemistry XXI*. Wiley: New York, 1990.
87. Southall NT, Dill KA, Haymet ADJ. A view of the hydrophobic effect. *J Phys Chem B.* 2002;106(3):521–533.
88. Meyer EE, Rosenberg KJ, Israelachvili J. Recent progress in understanding hydrophobic interactions. *Proc Natl Acad Sci USA.* 2006; 103(43):15739–15746.
89. Williams-Wynn MD, Letcher TM, Naidoo P, Ramjugernath D. Activity coefficients at infinite dilution of organic solutes in diethylene glycol and triethylene glycol from gas-liquid chromatography. *J Chem Thermodyn.* 2013;65:120–130.
90. Williams-Wynn MD, Letcher TM, Naidoo P, Ramjugernath D. Activity coefficients at infinite dilution of organic solutes in N-formylmorpholine and N-methylpyrrolidone from gas-liquid chromatography. *J Chem Thermodyn.* 2013;61:154–160.
91. McEwan BC. The mutual solubility of glycerol and alcohols, aldehydes, phenols, and their derivatives. *J Chem Soc Trans.* 1923;123: 2284–2288.
92. Furtado FA, Coelho GLV. Determination of infinite dilution activity coefficients using HS-SPME/GC/FID for hydrocarbons in furfural at temperatures of (298.15, 308.15, and 318.15) K. *J Chem Thermodyn.* 2012;49:119–127.
93. Cori L, Delogu P. Infinite dilution activity coefficients of ethanol-n-alkanes mixtures. *Fluid Phase Equilib.* 1986;27:103–118.
94. Domanska U, Lukoshko EV. Measurements of activity coefficients at infinite dilution for organic solutes and water in the ionic liquid 1-butyl-1-methylpyrrolidinium tricyanomethanide. *J Chem Thermodyn.* 2013;66:144–150.
95. Reza J, Trejo A. Temperature dependence of the infinite dilution activity coefficient and Henry's law constant of polycyclic aromatic hydrocarbons in water. *Chemosphere.* 2004;56:537–547.
96. Bamford HA, Poster DL, Baker JE. Temperature dependence of Henry's law constants of thirteen polycyclic aromatic hydrocarbons between 4°C and 31°C. *Environ Toxicol Chem.* 1999;18(9):1905–1912.
97. Krivokhizha SV, Lugovaya OA, Fabelinskiĭ IL, Chaĭkov LL. Miscibility dome of guaiacol-glycerin and increased transparency of heterogeneous solutions after shaking. *Sov Phys JETP.* 1985;62(1):48–51.

98. Christensen SP, Donate FA, Frank TC, LaTulip RJ, Wilson LC. Mutual solubility and LCST for water + glycol ether systems. *J Chem Eng Data.* 2005;50(3):869–877.
99. Frank TC, Donate FA, Merenov AS, Von Wald GA, Alstad BJ, Green CW, Thyne T. Separation of glycol ethers and similar LCST-type hydrogen-bonding organics from aqueous solution using distillation or liquid-liquid extraction. *Ind Eng Chem Res.* 2007;46(11): 3774–3786.
100. Parvatiker RR, McEwan BC. The mutual solubility of glycerol and amino- and hydroxyl- compounds. *J Chem Soc Trans.* 1925;124: 1484–1492.
101. Tumba K, Letcher TM, Naidoo P, Ramjugernath D. Activity coefficients at infinite dilution of organic solutes in the ionic liquid trihexyltetradecylphosphonium bis (trifluoromethylsulfonyl) imide using gas-liquid chromatography at T = (313.15, 333.15, 353.15, and 373.15) K. *J Chem Thermodyn.* 2013;65:159–167.
102. Kato S, Hoshino D, Noritomi H, Nagahama K. Determination of infinite-dilution partial molar excess entropies and enthalpies from the infinite-dilution activity coefficient data of alkane solutes diluted in longer-chain-alkane solvents. *Ind Eng Chem Res.* 2003; 42(20):4927–4938.
103. Thomas ER, Newman BA, Nicolaides GL, Eckert CA. Limiting activity coefficients from differential ebulliometry. *J Chem Eng Data.* 1982;27(3):233–240.
104. Yang Y, Wu H, Xie S. The measurement of activity coefficients at infinite dilution of binary volatile liquid systems by gas-liquid chromatography. *Chengdu Keji Daxue Xuebao.* 1983;5:27–32.
105. Yang Y, Xiao S, Li H, Fu Y. The measurement of infinite dilution activity coefficients by non-steady-state gas chromatography. *Chengdu Keji Daxue Xuebao.* 1988;10:35–38.
106. He Z, Fu H, Zhou X, Han S. New types of inclined ebulliometers for the determination of activity coefficients at infinite dilution. *Int Chem Eng.* 1991;31(1):171–177.
107. van Konynenburg PH, Scott RL. Critical lines and phase equilibria in binary van der Waals mixtures. *Philos Trans R Soc London A.* 1980;298:495–540.
108. Scott RL. Van der Waals-like global phase diagrams. *Phys Chem Chem Phys.* 1999;1(18):4225–4231.
109. Fileti EE, Chaudhuri P, Canuto S. Relative strength of hydrogen bond interaction in alcohol-water complexes. *Chem Phys Lett.* 2004;400:494–499.
110. Robeson LM. *Polymer Blends. A Comprehensive Review*. Carl Hanser Verlag: Munich, 2007.
111. Chatterjee S, Debenedetti PG. Fluid phase behavior of binary mixtures in which one component can have two critical points. *J Chem Phys.* 2006;124:154503.
112. Bai P, Keasler SJ, Siepmann JI. Liquid-liquid equilibria of binary water/1-butanol and water/THF mixtures studied by molecular simulation (208f). In: AIChE Annual Meeting, San Francisco, November 4, 2013.
113. Chen C-C, Simoni LD, Brennecke JF, Stadtherr MA. Correlation and prediction of phase behavior of organic compounds in ionic liquids using the nonrandom two-liquid segment activity coefficient model. *Ind Eng Chem Res.* 2008;47(18):7081–7093.
114. Moller B, Rarey J, Ramjugernath D. Extrapolation/interpolation of infinite dilution, activity coefficient as well as liquid and solid solubility between solvents: Part 1. Alkane solvents. *Fluid Phase Equilib.* 2014;361:69–82.
115. Doherty MF, Fidkowski ZT, Malone MF, Taylor R. Distillation. In: Section 13 in Green DW, editor. *Perry's Chemical Engineers' Handbook*, 8th ed. McGraw-Hill: New York, 2007.
116. Hwang Y-L, Olson JD, Keller II GE. Steam stripping for removal of organic pollutants from water. 2. Vapor-liquid equilibrium data. *Ind Eng Chem Res.* 1992;31(7):1759–1768.
117. Bhatia SR, Sandler SI. Temperature dependence of infinite dilution activity coefficients in octanol and octanol/water partition coefficients of some volatile halogenated organic compounds. *J Chem Eng Data.* 1995;40(6):1196–1198.
118. Smith FR, Harvey AH. Avoid common pitfalls when using Henry's law. *Chem Eng Prog.* 2007;103(9):33–39.
119. Brockbank SA, Giles NF, Rowley RL, Wilding WV. Predicting temperature-dependent aqueous Henry's Law constants using group contribution methods. *J Chem Eng Data.* 2014;59(4):1052–1061.
120. Sangster J. Octanol-water partition coefficients of simple organic compounds. *J Phys Chem Ref Data.* 1989;18(3):1111–1524.
121. Góral M, Wiśniewska-Gocłowska B, Mączyński A. Recommended liquid-liquid equilibrium data. Part 4. 1-Alkanol-water systems. *J Phys Chem Ref Data.* 2006;35(3):1391–1414.
122. Nagata I, Miyamoto K. Representation of mutual solubility data over a wide temperature range using a modified Wilson equation. *Thermochimica Acta.* 1992;205:307–317.
123. Wiśniewska-Gocłowska B, Malanowski SK. A new modification of the UNIQUAC equation including temperature dependent parameters. *Fluid Phase Equilib.* 2001;180:103–113.
124. Anonymous. *Aspen Physical Property System: Physical Property Models (Version 8.0)*. Aspen Technology: Cambridge, 2012.
125. Rawat BS, Gulati IB, Mallik KL. Study of some sulphur-group solvents for aromatics extraction by gas chromatography. *J Appl Chem Biotechnol.* 1976;26:247–252.

Appendix: Derivation of Equation 5

Equation 1, used to correlate $\gamma_{ij}^{\infty} = f(T)$, can be written as follows

$$\frac{\ln \gamma_{ij}^{\infty}(\text{at } T)}{\ln \gamma_{ij}^{\infty}(\text{at } T_1)} = \left(\frac{T_1}{T}\right)^{\theta_{ij}} \tag{A1}$$

where θ_{ij} is assumed to be constant. Rearranging to obtain an expression for $\ln \gamma_{ij}^{\infty}(T)$ yields

$$\ln \gamma_{ij}^{\infty}(\text{at } T) = {T_1}^{\theta_{ij}} \ln \gamma_{ij}^{\infty}(\text{at } T_1)\left(\frac{1}{T}\right)^{\theta_{ij}} \tag{A2}$$

Taking the derivative of $\ln \gamma_{ij}^{\infty}(T)$ with respect to $1/T$ and inserting the result into Eq. 3 yields

$$\begin{aligned} \left[\frac{\partial \ln \gamma_{ij}^{\infty}}{\partial(1/T)}\right]_{P,x} &= {T_1}^{\theta_{ij}} \ln \gamma_{i,j}^{\infty}(\text{at } T_1)\theta_{ij}\left(\frac{1}{T}\right)^{\theta_{ij}-1} \\ &= \theta_{ij} T_1 \ln \gamma_{i,j}^{\infty}(\text{at } T_1)\left(\frac{T_1}{T}\right)^{\theta_{ij}-1} = \frac{\overline{h}_{ij}^{E,\infty}}{R} \end{aligned} \tag{A3}$$

Equation A1 also can be written as

$$\frac{T \ln \gamma_{ij}^{\infty}(\text{at } T)}{T_1 \ln \gamma_{ij}^{\infty}(\text{at } T_1)} = \left(\frac{T_1}{T}\right)^{\theta_{ij}-1} \tag{A4}$$

Combining Eqs. A3 and A4 and rearranging yields Eq. 5, as follows

$$\frac{\overline{h}_{ij}^{E,\infty}}{R} = \theta_{ij} T_1 \ln \gamma_{ij}^{\infty}(\text{at } T_1)\frac{T \ln \gamma_{ij}^{\infty}(\text{at } T)}{T_1 \ln \gamma_{ij}^{\infty}(\text{at } T_1)} = \theta_{ij} T \ln \gamma_{ij}^{\infty}(\text{at } T) \tag{A5}$$

$$\overline{h}_{ij}^{E,\infty} = \theta_{ij} R T \ln \gamma_{ij}^{\infty} \tag{A6}$$

Manuscript received Apr. 7, 2014, and revision received June 30, 2014.